The anatomy and ontogeny of modern intra-oceanic arc systems

ROBERT J. STERN

Geosciences Department, University of Texas at Dallas, Richardson, TX 75083-0688, USA
(e-mail: rjstern@utdallas.edu)

Abstract: Intra-oceanic arc systems (IOASs) represent the oceanic endmember of arc–trench systems and have been the most important sites of juvenile continental crust formation for as long as plate tectonics has operated. IOASs' crustal profiles are wedge-shaped, with crust up to 20–35 km thick; a more useful definition is that IOASs occur as chains of small islands, generally just the tops of the largest volcanoes. A very small fraction of IOASs lie above sea level, but advancing marine technologies allow their most important features to be defined. Modern IOASs subduct old, dense oceanic lithosphere and so tend to be under extension. They consist of four parallel components: trench, forearc, volcanic–magmatic arc, and back-arc, occupying a $\geq$200 km zone along the leading edge of the overriding plate. These components form as a result of hydrous melting of the mantle and reflect the strongly asymmetric nature of subduction processes. Forearcs preserve infant arc lithosphere whereas magmatism in mature IOASs is concentrated along the volcanic–magmatic front. Mature IOASs often have minor rear-arc volcanism and, because most IOASs are strongly extensional, sea-floor spreading often forms back-arc basins. Sub-IOAS mantle is also asymmetric, with serpentinized harzburgite beneath the forearc, pyroxene-rich low-V_p mantle beneath the magmatic front, and lherzolite–harzburgite beneath back-arc basins. Because most IOASs are far removed from continents, they subduct oceanic lithosphere with thin sediments and have naked forearcs subject to tectonic erosion. IOASs evolve from broad zones of very high degrees of melting and sea-floor spreading during their first 5–10 Ma, with the volcanic–magmatic front retreating to its ultimate position *c.* 200 km from the trench.

Continental crust is basically a mosaic of orogenic belts, and these in turn are largely nests of island arcs, welded and melded together. Arcs are what is produced in the overriding plate of a convergent margin when subduction is sufficiently rapid (faster than *c.* 2 cm a^{-1}) for long enough that the subducted plate reaches magmagenetic depths (100–150 km) and causes the mantle to melt. This configuration must exist for long enough that melts generated in the overlying asthenospheric wedge not only reach the surface but also persist until a stable magmatic conduit system is established. When this happens, magma produced by hydrous fluxing of the mantle will rise towards the surface to form volcanoes and plutons of a magmatic arc. This magmatic locus and its often spectacular volcanoes are important parts of an arc, but neovolcanic zones make up a relatively minor part of any arc. Arcs can be built on continental or oceanic lithosphere. Here the focus is on those arcs that are built on oceanic crust, which may be called intra-oceanic arc systems (IOASs). These can be distinguished from arcs built on continental crust, also known as 'Andean-type arcs'.

IOASs are constructed on thin, mostly mafic crust, and consequently these magmas are not as contaminated by easily fusible felsic crust as are magmas from Andean-type margins, which are built on much thicker and more felsic continental crust (Fig. 1). IOASs are widely acknowledged as sites where thickened welts of juvenile (i.e. derived from melting of the mantle) crust is produced. In spite of this significance, IOASs are significantly less well studied than Andean-type arcs. The main reason for this is that the vast bulk of IOASs are submerged below sea level and difficult to study. Nevertheless, our understanding of IOASs has advanced greatly since these were first reviewed a quarter of a century ago by Hawkins *et al.* (1984); an overview of arcs in general was also prepared about that time (Hamilton 1988). New developments in marine technology [global positioning system (GPS), sonar swathmapping, deep-sea drilling, manned submersibles, remotely operated vehicles (ROVs) and autonomous underwater vehicles (AUVs)] are allowing the study of IOASs to advance rapidly, and we now have a good grasp of their most important features. The purpose of this paper is to summarize our understanding of IOASs for a broad geoscientific audience, with the hope that this understanding will allow geologists studying ancient crustal terranes to better identify fossil IOASs in orogens and cratons. This review draws heavily on 30 years of studying the Izu–Bonin–Mariana arc system, especially the Marianas, and examples are drawn heavily from this IOAS. The general tectonic and magmatic relationships observed there are mostly

From: KUSKY, T. M., ZHAI, M.-G. & XIAO, W. (eds) *The Evolving Continents: Understanding Processes of Continental Growth*. Geological Society, London, Special Publications, **338**, 7–34.
DOI: 10.1144/SP338.2 0305-8719/10/$15.00

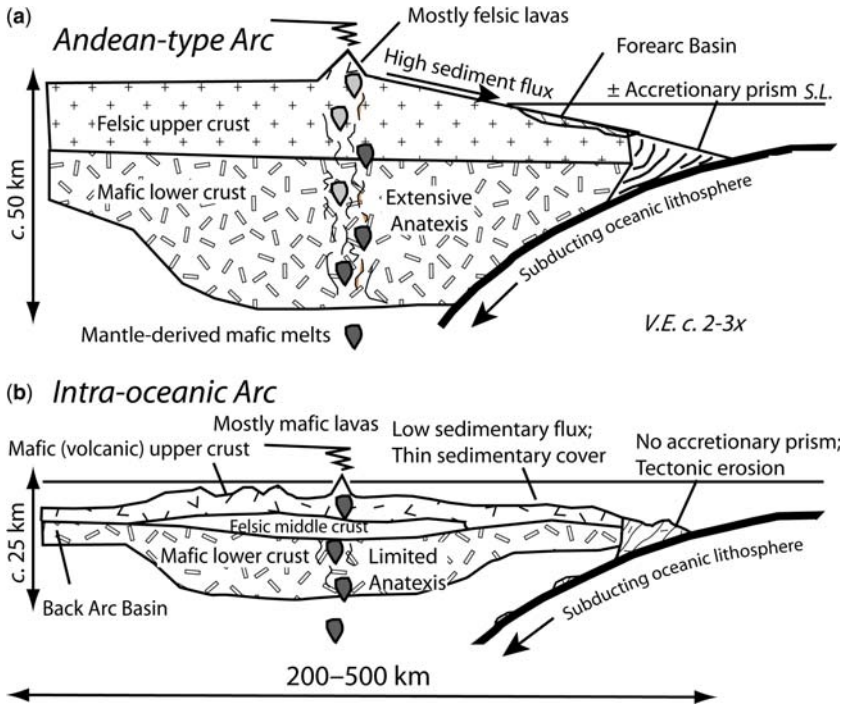

Fig. 1. Comparison of Andean-type arc (**a**) and intra-oceanic arc system (**b**), greatly simplified.

applicable to the general case of modern IOAS formation and evolution.

What is an intra-oceanic arc system?

Arc–trench systems comprise the lithosphere (crust and uppermost mantle) between the trench and the back-arc region. IOASs are one endmember in the spectrum of arc–trench systems, the opposite end of the spectrum from Andean-type arcs. This spectrum reflects differences in what the arc is constructed on and thus its crustal composition, thickness, and elevation. IOASs are built on oceanic crust, whereas Andean-type arcs are built on pre-existing continental crust. Correspondingly, IOAS crust is thinner and more mafic than that beneath Andean-type arcs, which is thicker and more felsic (Fig. 1). This reduces the opportunity for primitive, mantle-derived magmas to interact with the crust en route to the surface; consequently, IOAS lavas are less differentiated, more mafic, and less contaminated than are lavas erupted from Andean-type arcs. The more primitive nature of IOAS igneous rocks better preserves evidence of the subduction-modified mantle-derived melts that formed them than do igneous rocks from Andean-type arcs, and this 'window on subduction-zone processes' is a paramount reason that studies of IOAS arcs are advancing rapidly (although it must be noted that all arc lavas tend to be more fractionated than are mid-ocean ridge basalt (MORB) or 'hotspot' lavas).

IOASs are the fundamental building blocks that are assembled over geological time into orogens, cratons, and continents. If the continental crust can be likened to a brick wall, then an IOAS plays the role of a single brick. This analogy has limited utility, because bricks in a wall and IOASs look and behave very differently. First, bricks are homogeneous, whereas IOASs are heterogenous, with significant vertical and transverse compositional variations, both in the crust and in the mantle lithosphere. Second, bricks are annealed solid aggregates, whereas IOASs form from melts and continue through their lives to interact with mantle-derived melts as well as generating eutectic crustal melts. Continued magmatic additions to the base of IOAS occurs across a 'transparent Moho', with some mantle-derived melts permeating or traversing the crust whereas others are underplated to the base of the crust, at the same time that dense cumulates and residues 'delaminate' or sink back into the convecting asthenosphere. Third, bricks are rectangular parallelepipeds, or cuboids, whereas IOAS crust has the relative dimensions of flattened noodles: much

wider (*c.* 250 km) than thick (15–35 km), much longer (hundreds to thousands of kilometres) than wide. Finally, bricks cemented into a wall are inert and immutable, whereas juvenile crust composed of accreted IOASs continues to deform as well as interact with and generate melts long after these are accreted. These melts, continuing deformation, and attendant metamorphism serve as the cement that welds different IOASs together.

IOASs are built on oceanic crust, but this crust generally forms when subduction begins, as discussed below. Crustal thicknesses are typically 20–35 km beneath the magmatic arc, thinning beneath the back-arc region and tapering trenchward. Detailed seismic studies of arcs are needed to actually measure crustal thicknesses, and these are relatively uncommon (the western Aleutian and Izu–Bonin–Mariana arcs are the IOASs with the best-imaged crustal structure; see Stern *et al.* 2003). However, the relative paucity of geophysical soundings of arcs does not seriously impede our ability to identify these among Earth's inventory of convergent margins. Because crustal thickness typically is reflected in elevation, intra-oceanic arcs are generally mostly below sea level. This serves as a useful (and simple) criterion for identifying intra-oceanic arcs: if much of the volcanic front of a given arc system lies below sea level, it can usefully be described as an intra-oceanic arc. Similarly, if the volcanic front of a given arc mostly lies above sea level, this is probably an Andean-type arc. This twofold classification differs from the threefold subdivision of de Ronde *et al.* (2003), who identified: (1) intra-oceanic arcs (those with oceanic crust on either side); (2) transitional or island arcs (those along the margins of island chains with a basement of young continental crust); (3) continental arcs (those developed along the margins of continents). De Ronde *et al.*'s (2003) intermediate category of 'island arc' is the principal difference, and although I agree that arcs built on crust that is transitional between true oceanic and continental crusts exist (e.g. the Philippines), assignment to this intermediate group requires more information about the nature of crustal substrate than is commonly available. Figure 2 shows the distribution of IOASs as they are identified here.

IOASs tend to form where relatively old oceanic crust, generally Cretaceous or older, is subducted. Such lithosphere is negatively buoyant, which causes the subducting sea floor to sink vertically as well as subduct down-dip, in turn causing the trench (and the associated arc system) to 'rollback' (Garfunkel *et al.* 1986; Hamilton 2007). Such a situation favours development of convergent plate margins within the oceanic realm and thus IOASs. In contrast, subduction of young oceanic lithosphere engenders a strongly compressional convergent margin so that the arc system migrates away from the ocean basin and onto any flanking continent. Subduction of older oceanic lithosphere favours development of an overall extensional strain regime in the hanging wall of the associated convergent margin and is an important reason why IOASs tend to be associated with back-arc basins, discussed further below.

It is essential to distinguish between the early stages in the formation of an IOAS and its subsequent evolution. The latter stages are usefully referred to as 'mature', and all of the IOASs that

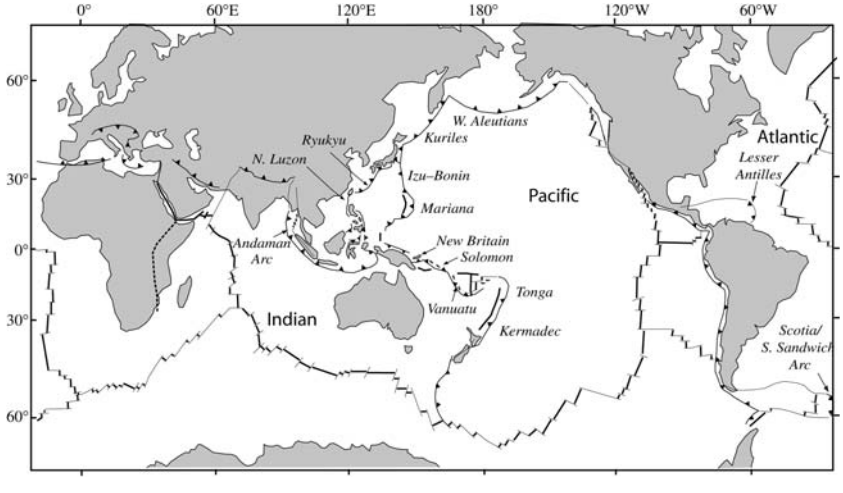

Fig. 2. Location of convergent plate margins and distribution of intra-oceanic arc systems.

are active today are in this stage. An IOAS changes somewhat once it becomes mature, but these changes are episodic as well as progressive. Episodic changes include the formation of back-arc basins and tectonic erosion of the forearc. Progressive changes include thickening of the crust beneath the volcanic–magmatic front, extent of serpentinization of subforearc mantle, and the thickness of sediments that are accumulated. The early stages in the life of an IOAS are called 'infant', 'nascent', or 'immature' and few of the characteristics of mature IOASs pertain to this stage. The infant arc stage is relatively brief, lasting *c.* 5–10 Ma. Because none of the currently active IOASs are in this stage, our understanding of infant arcs is reconstructed from mostly early Cenozoic examples in the Western Pacific, especially the Izu–Bonin–Mariana arc. Except for the final section 'IOAS forearc structure preserves its early history', this review concentrates on mature IOASs.

How do we know about intra-oceanic arc systems?

Because arcs are large and heterogeneous geological entities, their study involves the full range of geoscientific perspectives: geochemistry, sedimentology, geophysics, geodynamics, structure, metamorphism, palaeontology, etc. Such studies of IOASs are more difficult in many ways than those of Andean-type arcs, simply because the former are largely below and the latter largely above sea level. Consequently, submarine geological studies are much more expensive than studies on land. It is only when studying the trench and deeper parts of the forearc (which are submerged for both Andean-type and intra-oceanic arc systems) that the same marine geological approaches must be used. Also, Andean-type arcs lie near many population centres and pose serious volcanic, landslide, and seismic hazards (also benefits such as geothermal energy and mineral deposits), whereas IOASs are isolated, sparsely populated, and any mineral deposits are difficult to exploit. Because traditional land-based geoscientific approaches can be used to study Andean-type arcs, and because many nations rightfully have concerns for the public good, studies of such systems and our understanding of them are relatively advanced. Some geoscientific work on IOASs can be done above sea level but this is limited to the upper slopes of the tallest volcanoes and isolated structural highs. Understanding IOASs requires using research vessels and marine geotechnology, which are expensive. Our understanding of IOASs naturally lags behind that of Andean-type margins but is advancing rapidly.

Intra-oceanic arc-itecture

At broad scale, IOASs consist of four components, as shown in Figure 3: trench, forearc, volcanic–magmatic arc, and back-arc. These same components are just as useful for subdividing the transverse structure of Andean-type arc-trench systems. IOASs are often associated with back-arc basins, where sea-floor spreading occurs, or with narrower rift zones. Other IOASs show no evidence of extension, but no modern IOAS is associated with back-arc shortening. Further details about these four components are provided below.

Trench

The trench marks where the two converging plates meet. Because one plate bends down to slide beneath the other, trenches are global bathymetric lows, several thousands of metres deeper than sea floor away from the trench. A trench can be filled with sediments or contain very little sediment, depending on how much is supplied to it. Sediment flux reflects proximity to continents. Trenches associated with Andean-type arcs can receive large volumes of sediments delivered by rivers or glaciers and thus are often filled. In contrast, very few of the trenches associated with IOASs contain significant sediment. The only IOAS trenches with significant sediment fill are found in the southernmost Lesser Antilles, where the Orinoco River delta lies at the southern terminus of this trench, the Aleutians, where sediment from Alaskan glaciers and rivers flows longitudinally westwards along the trench, and in the Andaman–Nicobar region, where the trench is fed by the Ganges–Brahmaputra river system. The sediment volume in the trench controls whether or not the forearc is associated with a significant accretionary prism (Clift & Vannucchi 2004; Scholl & von Huene 2007). Because most IOAS trenches are starved of sediment, accretionary prisms are not generally found in the inner trench

Fig. 3. (**a**) Schematic section through the upper 140 km of an intra-oceanic arc system (with an actively spreading back-arc basin), showing the principal crustal and upper mantle components and their interactions. It should be noted that the 'mantle wedge' (unlabelled) is that part of the asthenosphere beneath the magmatic front. The mantle between the asthenosphere and the trench is too cold to melt (modified after Stern *et al.* 2003). (**b**) Typical intra-oceanic forearc (modified after Reagan *et al.* (2010)). The exposed ophiolitic basement, thin sediments, absence of accretionary prism, and deep, empty trench should be noted (**c**) Crustal structure beneath the volcanic–magmatic front of a typical

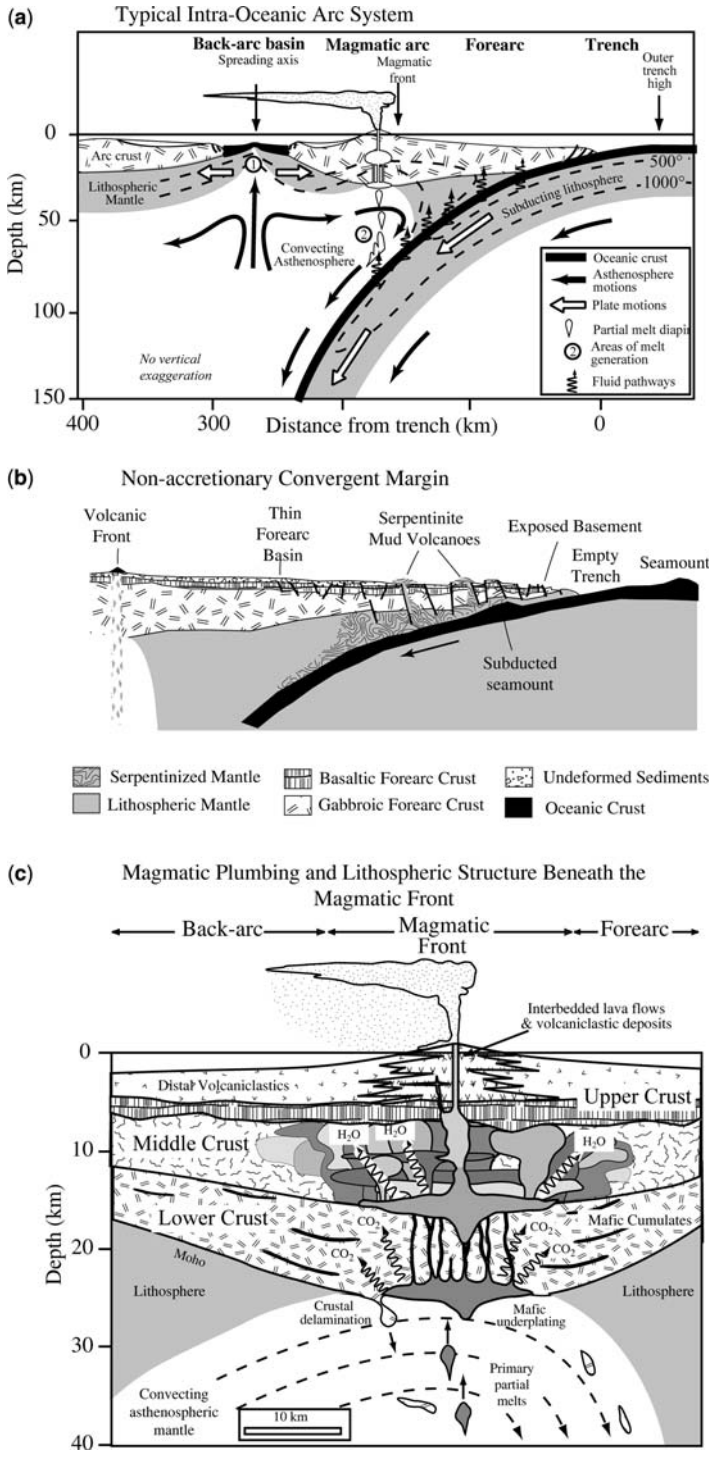

Fig. 3. (*Continued*) intraoceanic arc (modified after Stern 2003). The asthenosphere is shown extending up to the base of the crust; delamination or negative diapirism is shown, with blocks of the lower crust sinking into and being abraded by convecting mantle. Regions where degassing of CO_2 and H_2O is expected are also shown.

wall of IOASs, with the exceptions noted above. Instead, igneous basement, generally basalt, boninite, diabase, gabbro and serpentinized peridotite, is exposed in the inner trench wall (Reagan *et al.* 2010). These rocks make up an *in situ* ophiolite, produced when subduction began, as discussed below. Such exposures are important sources of information about the nature of forearc crust, along with drilling and geophysical studies (Clift & Vannucchi 2004; Scholl & von Huene 2007).

IOAS inner trench walls are highly fractured by continuing deformation and earthquakes associated with plate convergence. Subduction of seamounts and other bathymetric highs further fracture the inner trench wall. The cumulative effect is that much of the inner trench wall slope is defined by the angle of repose for fractured igneous rocks, especially at its base. The base of the inner trench wall consists of a talus prism of this material. This loose talus is carried into the subduction zone, resulting in significant 'tectonic erosion' of the outer forearc.

Forearc

The forearc is the lithosphere that lies between the trench and magmatic arc, generally 100–200 km wide. Its most important characteristic is a lack of recent igneous activity and remarkably low heat flow, even though forearc crust preserves strong evidence that igneous activity of unusual intensity occurred when subduction began. Morphologically, the forearc slopes gently towards the trench. It can be subdivided into a more stable inner forearc and a more deformed outer forearc. Tectonically stable forearcs, such as the Izu forearc, are also commonly deeply incised by submarine canyons. In contrast, actively deforming forearcs, such as the Mariana forearc, generally lack a well-developed canyon system.

Geophysical soundings of a typical IOAS forearc such as that of Izu–Bonin–Marianas reveal a predominantly mafic crust that tapers towards the trench, such that mantle peridotite is often exposed in the inner trench wall (Fisher & Engel 1969; Bloomer & Hawkins 1983; Pearce *et al.* 2000). *P*-wave velocities increase vertically downward from V_p consistent with fractured basaltic and boninitic lavas to V_p consistent with diabase and gabbro (Figs 4 & 5). This *P*-wave velocity structure is similar to that of oceanic crust or ophiolites, consistent with sampling of the IOAS inner trench walls. The significance of the ophiolitic nature of IOAS forearc crust is explored further in the final section 'IOAS forearc structure preserves its early history'.

The upper mantle beneath IOAS forearc crust is serpentinized, as demonstrated by low seismic velocities and the presence of serpentinite mud volcanoes in the outer forearc of at least one IOAS, the Marianas (Stern & Smoot 1998; Oakley *et al.* 2007). The extent of serpentinization seems to vary with distance from the trench; rocks are more serpentinized towards the trench, and less serpentinized away from it. This is shown by upper mantle P-wave velocities, which decrease significantly from V_p *c.* 8.1 km s^{-1} beneath the inner forearc to 6.4 km s^{-1} towards the trench. The greater serpentinization beneath the outer compared with the inner forearc makes the outer forearc weaker and easier to deform. Forearc mantle is composed of strongly depleted harzburgite, characterized by spinels with Cr-number $[= 100\mathrm{Cr}/(\mathrm{Cr} + \mathrm{Al})] > 50$ (Bloomer & Hawkins 1983; Parkinson & Pearce 1998; Okamura *et al.* 2006).

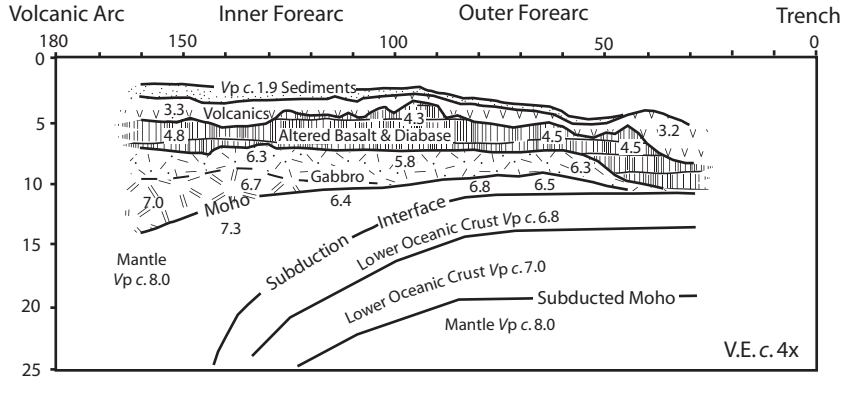

Fig. 4. Simplified *P*-wave velocity structure beneath Izu forearc (roughly east–west line at 30°50′E) modified after Kamimura *et al.* (2002), with interpreted lithologies. Forearc crustal thickness decreases from *c.* 11 km near the volcanic arc to 5 km or less near the trench. Also, V_p is significantly lower in uppermost mantle beneath the outer forearc (6.4–6.8 km s^{-1} v. 7.3–8.0 km s^{-1}), probably reflecting greater serpentinization beneath the outer forearc.

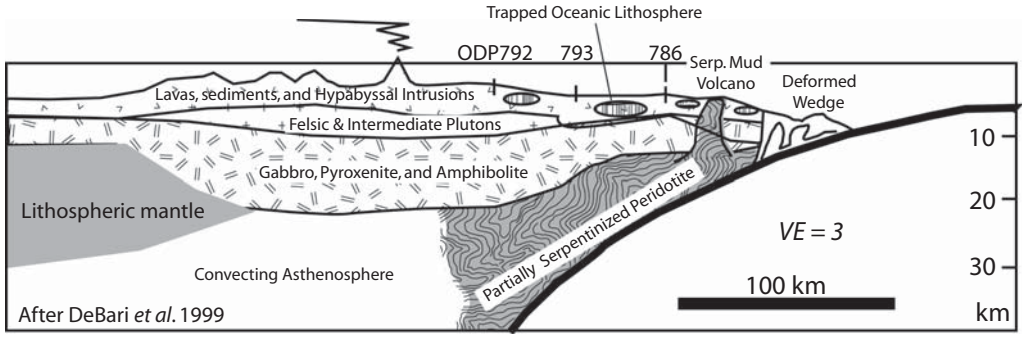

Fig. 5. Interpretation of the seismic structure of the crust and upper mantle of a typical intra-oceanic arc, modified after DeBari *et al.* (1999). This section is interpreted from the seismic refraction study of Suyehiro *et al.* (1996) for the Izu arc. The presence of a mid-crustal 'tonalite' layer should be noted.

Sediments are a relatively unimportant part of the forearc, but there are some. The relatively stable inner forearc may host a thin forearc basin, with a few hundred metres to few kilometres of sediment thickness. This paucity of sediment in IOAS forearcs is consistent with the fact that IOAS trenches are empty, and contrasts with the robust accretionary prisms and thick forearc basins characteristic of many Andean forearcs.

Volcanic–magmatic arc

The locus of continuing igneous activity in a mature IOAS defines the magmatic arc. This is recognized in modern IOASs as a linear or arcuate array of volcanoes that parallel the trench (England *et al.* 2004; Syracuse & Abers 2006). These are the largest and most productive volcanoes in a mature IOAS and are often the only feature that rises above sea level. These volcanoes are underlain by plutons and hypabyssal intrusions exposed by erosion in ancient, fossil IOASs. The trenchward limit of young igneous activity is referred to as the 'volcanic front' or 'magmatic front', and marks a steep gradient in heat flow, which is low towards the trench and high towards the back-arc region. The style of IOAS volcanism is fundamentally different from that of the other two great classes of oceanic volcanism, mid-ocean ridges and hotspots. Mid-ocean ridge volcanism is entirely volatile-poor tholeiitic basalt, which produces crust of nearly constant thickness (5–7 km) when magma fills the gap between two plates being pulled apart. Hotspot volcanism typically builds a linear chain of tholeiitic and/or alkalic lavas, with a progression of ages that increases in the direction of plate motion; generally only a volcano or two at one end of the hotspot chain are active. IOAS volcanoes, in contrast, remain relatively fixed with respect to the trench, so that the crust thickens at a rate of several hundred metres per million years as a result of the cumulative effects of magmatic addition at essentially the same place. Furthermore, IOAS magmas are relatively rich in silica and in volatiles, especially water, so that these eruptions are more violent and lavas are dominated by fragmental material, except in deep water, where the pressure suppresses violent degassing of magmas. This can sometimes be seen in the deposits of a growing IOAS volcano, as it grows from a base at 2–4 km below sea level to shallower water and then becomes an island. Eruptions from such a volcano are likely to change progressively with time from more effusive flows to increasingly fragmental as eruptions occur at increasingly lower *P* environments over time.

Hydrothermal activity and ore deposits associated with IOASs are also distinct from those associated with other oceanic igneous settings. Hydrothermal mineralization at mid-ocean ridges is controlled by the heating of seawater by hot rocks, which sets up a hydrothermal circulation that also leaches metals from the fractured basalts as it passes through these; these dissolved metals precipitate when hydrothermal fluids vent on the sea floor. Such circulation and leaching also occurs in association with IOAS submarine volcanoes, but in addition, the volatile-rich nature of IOAS magmas contributes directly to mineralization when these magmas degas (de Ronde *et al.* 2003; Baker *et al.* 2005). There are thus fundamental differences expected for mineral deposits that are related to mid-ocean ridges and IOASs.

IOAS arc volcanoes are built on a platform that varies in depth but that is characteristically well below sea level. The depth of this platform depends mostly on crustal thickness, and is shallower above thicker arc crust and deeper above

thinner arc crust. Correspondingly, whether or not IOAS volcanoes rise above sea level depends not only on the size of the volcano (reflecting age and magma production rate) but also the thickness of the underlying crust. There is no characteristic spacing between volcanoes along the magmatic front (d'Ars *et al.* 1995). Where the sea floor has been imaged between volcanoes, there is little evidence of young lavas.

IOAS volcanoes erupt mostly basalts but these are distinct because they are characteristically vesicular, porphyritic, and fractionated. This is evidence that one or more magma reservoirs exist within the arc crust, as depicted in Figure 3c. Processing of magmas and crust in the middle crust is probably responsible for the formation of tonalitic middle crust. Thus IOAS crust thickens by addition of lavas on top as well as plutonism within the crust. IOAS crustal growth is discussed further below. Felsic magmas also erupt in IOASs, usually from large, submarine calderas. Such submarine calderas are now well documented in the Izu and Kermadec IOASs (Fiske *et al.* 2001; Graham *et al.* 2008). The origin of felsic melts in IOASs is controversial, and partly depends on the nature of lower arc crust, as discussed below.

IOAS magmatic arcs show strong asymmetries in the volume and composition of magmatic products. Melts along the volcanic–magmatic front reflect the highest degree of melting and much larger volcanoes compared with those at a greater distance from the trench.

Back-arc basins and intra-arc rifts

Convergent margins can show extension or contraction, or be strain-neutral. These strain regimes are most clearly manifested in back-arc regions. More often than not, IOASs are associated with active back-arc basins (BABs); such arcs include the Marianas (Mariana Trough; Fig. 7), Tonga–Kermadec (Lau–Havre Basin), New Britain (Manus Basin), Vanuatu (North Fiji Basin), Andaman–Nicobar (Andaman Sea), and South Scotia (East Scotia Basin), so this is shown as part of a typical IOAS in Figure 3a. Other IOASs are associated with extinct BABs, including the Lesser Antilles, Western Aleutians, and Izu–Bonin arcs. Active BABs form by sea-floor spreading, which can be fast (>10 cm a^{-1}) or slow (1–2 cm a^{-1}; Stern 2002; Martinez & Taylor 2003). Spreading results from extensional stresses that split the arc, mostly as a result of to trench rollback. Rifting to initiate a BAB can begin in the inner forearc, along the arc, or immediately behind the arc, as summarized in Figure 6. In any case, arc igneous activity may be extinguished temporarily as mantle-derived magmas are captured by the extension axis. The rifted part of the arc is progressively separated from the volcanic–magmatic front, forming a remnant arc that subsides as spreading continues (Karig 1972). BAB spreading produces sea floor with a crustal structure that is largely indistinguishable from that produced by mid-ocean ridges. Inter-arc rifts create significant basins within IOASs but no sea-floor spreading. These may or may not evolve into BABs; typical examples of inter-arc rifts are found in the Izu and Ryukyu arcs.

IOAS sediments

As mentioned before, IOASs are characterized by slow sedimentation rates and relatively thin sediments. Unless an IOAS lies near a continent, its trench will be empty and it will not have an accretionary prism. Significant sediment accumulations in IOASs occur only near the volcanic front, both on the back-arc side and forearc side. Sedimentation rates here will also reflect prevailing wind directions, which control the direction of volcanic ash dispersal and which flanks of subaerial volcanoes will be preferentially eroded by waves. Larger volcanoes are increasingly affected by flank collapse, which episodically sends tremendous volumes of sediment downslope.

Two sites of sedimentary basins in IOASs are worthy of further discussion: the forearc basin and the BAB immediately adjacent to the volcanic arc. Figure 8 shows typical examples of both, using a *c.* 350 km long multi-channel seismic reflection profile across the Mariana arc–trench system.

Most IOASs have an elongated basin parallel to the volcanic arc on the inner forearc. Such forearc basins are 50–80 km wide (Chapp *et al.* 2008). Sediments in the Mariana forearc basin have a maximum thickness of 1.5 s (two-way travel time; Fig. 8). Deep Sea Drilling Project (DSDP) Site 458 drilled into the distal edge of this forearc basin, penetrating *c.* 250 m of Oligocene–Pleistocene sediments and into Eocene basement (Shipboard Scientific Party 1982*b*). Physical property measurements indicate $V_p < 2.0$ km s^{-1} for these sediments, implying a maximum thickness of *c.* 1.5 km for this basin. These sediments have accumulated over the past 35 Ma, implying a maximum sedimentation rate of *c.* 43 m Ma^{-1}.

The other important sedimentary basin lies at the juncture between thin BAB crust and thicker crust beneath the volcanic–magmatic arc (Fig. 7). This results in a deep basin where arc-derived volcaniclastic sediments are deposited. In the case of the Mariana Trough profile shown in Figure 8, the sediments are <0.75 s thick. DSDP Site 455 drilled *c.* 100 m into a similar sediment pile just to the north of this profile (Shipboard Scientific Party

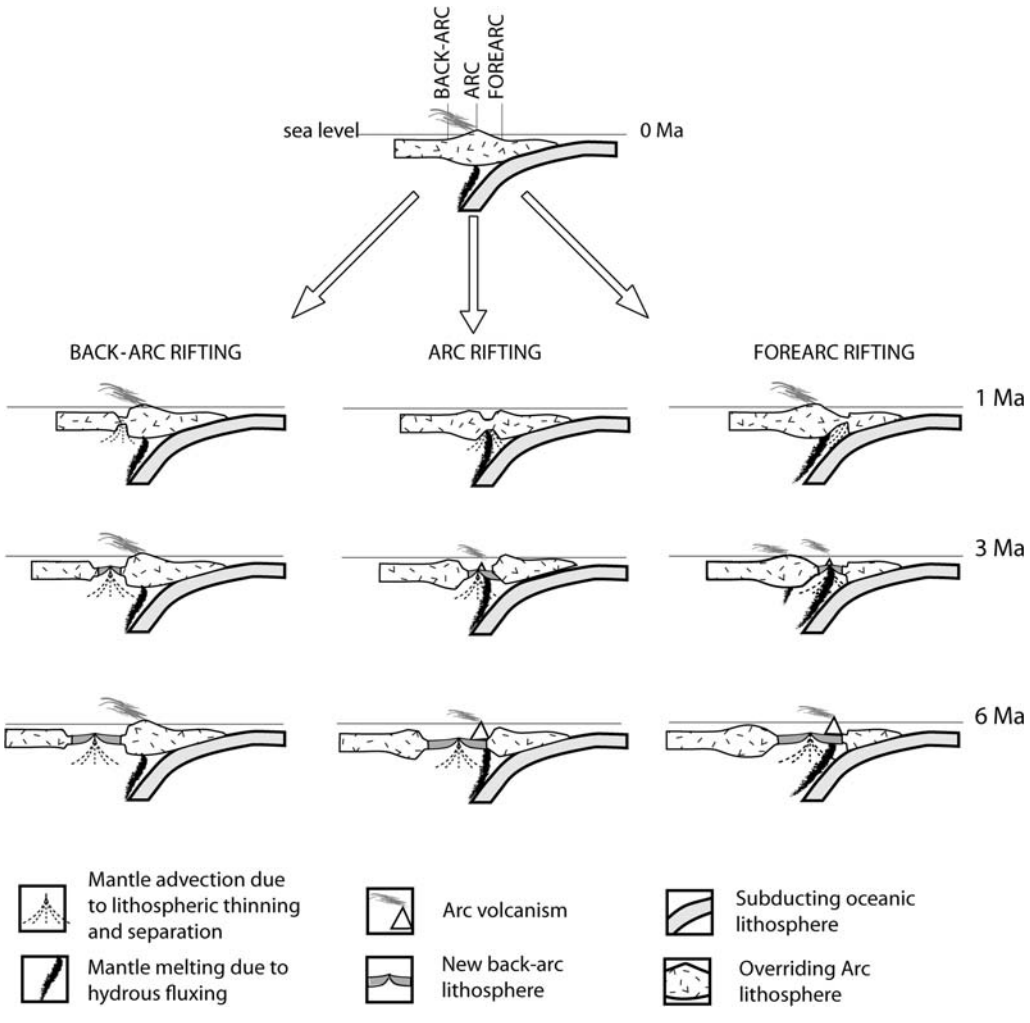

Fig. 6. Three ways in which an IOAS can rift to form a back-arc basin, modified after Martinez & Taylor (2006). The initial slab and arc lithospheric geometry is shown at the top. The three sets of panels depict the evolving geometry and interaction with arc melt sources (tied to the subducting slab) and back-arc melt generation (tied to mantle advection driven by separation of the overriding lithosphere). Left panels show BAB formation by rifting behind the active magmatic arc, in which case arc volcanism will not be interrupted and a narrow, thin remnant arc is produced. The middle panels show BAB formation by rifting the active arc, whereby the arc magmatic budget will initially be captured by the extension axis, shutting down the arc and forcing re-establishment of a new magmatic arc. The right panels shows BAB formation by forearc rifting, whereby the active magmatic arc will slowly migrate away from above the site of melt generation in the mantle and be extinguished, at the same time as a new magmatic arc forms above the site of mantle melt generation. In this case, a very broad and thick forearc is formed.

1982*a*) and DSDP Site 456 (about 20 km farther west, near the distal edge of the BAB sedimentary basin) penetrated 170 m of sediment and into BAB basaltic crust. Physical property measurements indicate V_p *c.* 2 km s^{-1} for DSDP 455 sediments, indicating a maximum thickness of *c.* 750 m. These sediments have accumulated over the past 7 Ma (since the Mariana Trough back-arc basin began to open), implying a maximum sedimentation rate of *c.* 100 m Ma^{-1}. The greater sedimentation rate for the back-arc basin adjacent to the arc relative to the forearc basin sedimentation rate reflects the fact that this basin is closer to the active arc than the forearc basin, which is separated from

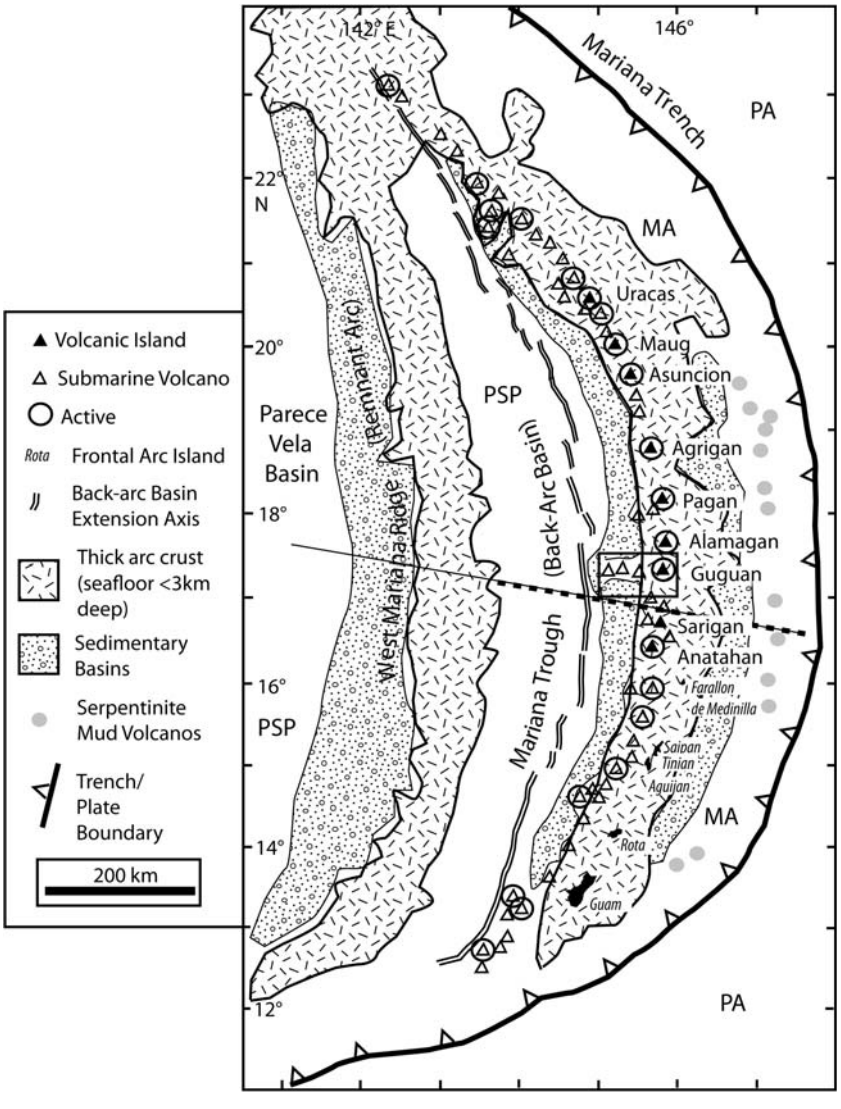

Fig. 7. Simplified tectonic map of the Mariana IOAS, showing the distribution of active arc volcanoes, back-arc basin spreading ridge (modified after Baker *et al.* 2008), frontal arc uplifted islands, remnant arc, major sedimentary basins, and serpentinite mud volcanoes (P. F. Fryer, pers. comm.). Location of boundaries between subducting Pacific plate (PA) and overriding Mariana plate (MA) and Philippine Sea plate (PSP) are also shown. Dashed line shows location of multichannel seismic profile shown in Figure 8; collinear fine continuous line shows position of lithospheric sounding profile in Figure 13. Box shows location of HMR-1 sonar image shown in Figure 9.

the active arc by the frontal arc structural high. Neither basin shows sedimentation rates that are particularly impressive.

Sediments in the Mariana forearc and back-arc basins are dominantly volcanogenic and derived from the active volcanic arc. These basins have sea floor that lies *c.* 3–4 km below sea level, mostly above the carbonate compensation depth so that carbonate sediments could be preserved, but biological productivity in this part of the ocean is low and biogenic sediments form a minor part of the fill of either basin. Forearc and back-arc basin sedimentation where biological productivity is higher (at high latitudes and equatorial regions) may have considerably larger proportions of biogenic components (Marsaglia 1995).

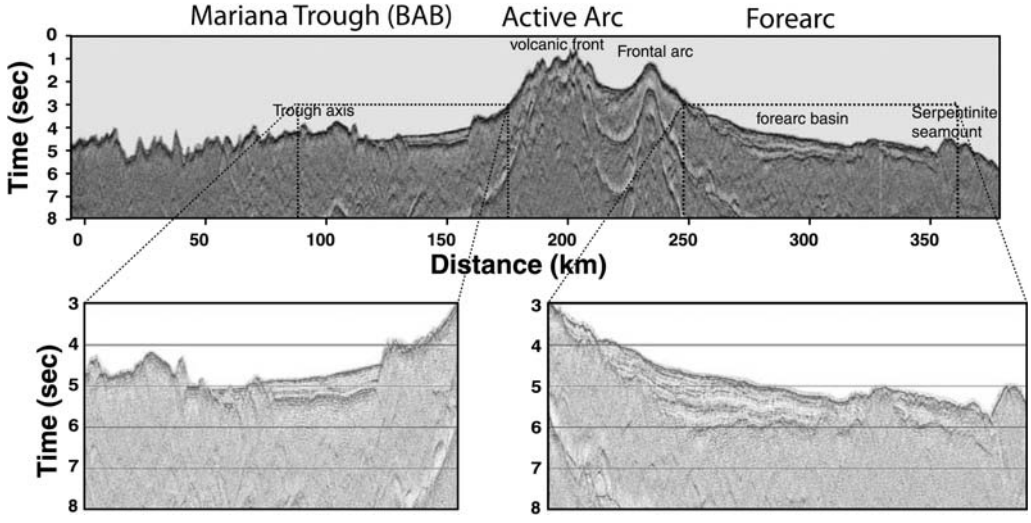

Fig. 8. Multi-channel reflection profile across the Mariana arc, from trench to back-arc basin, from Takahashi *et al.* (2008) with permission. Multiples should be noted. Location shown in Figure 7.

Volcanogenic sediments are transported from the active arc to forearc and back-arc basins probably by turbidity currents and by ash settling out of the water column. Many IOAS volcanoes are surrounded by submarine giant dunes, with wavelengths of up to 2 km, which define proximal sediment aprons that extend up to 60 km. The origin of these is poorly understood (Embley *et al.* 2006). Much other sediment must be transported by turbidites. Sonar backscatter images reveal well-developed, sinuous channels up to 100 km long, flowing downslope from the base of Mariana arc volcanoes towards the BAB to the west (Fig. 9). These may have evolved to transport turbidites produced by collapse of oversteepened arc volcano slopes, allowing mobilized sediments to move to depocentres in the eastern part of the Mariana Trough BAB. The relatively shallow depth of the BAB spreading ridge effectively partitions the two sides of any BAB into a sediment-starved portion that is distal to the active volcanic arc and an arc-proximal portion that is sediment-filled.

IOAS melts, lavas, and plutons

IOAS lavas are characteristically subalkaline and dominated by basalts and their fractionates. High-Mg andesites and rhyodacitic magmatic products also occur (Kelemen *et al.* 2003), with a minor amount of shoshonitic lavas in some cross-chains and along tectonically complex magmatic fronts. Boninites sometimes are formed when subduction zones begin. Tholeiitic basalts dominate BAB lavas, but the terms 'tholeiitic', 'calc-alkaline' and 'high-alumina basalt' all are used to describe the dominant IOAS volcanic front lavas. Arculus (2003) criticized especially the way that the term 'calc-alkaline' is commonly used, and proposed a new classification scheme for convergent margin igneous rocks. This scheme recognizes the importance of oxygen fugacity in controlling FeO^T/MgO v. silica variations in arc lavas as a complement to already established potassium–silica variations (high-Fe, medium-Fe, and low-Fe along with high-K, medium-K, and low-K suites).

The composition of these rocks reflect the unusual nature of subduction-related magmatic processes that make IOAS magmas. These begin with progressive metamorphism and perhaps melting of water-saturated subducted sediments, altered oceanic crust, and serpentinites as these are squeezed and heated in the subduction zone. Increasing pressure and heat closes fractures and pores, then dehydrates hydrous minerals. The result is a continuous release of water during progressive metamorphism to denser and drier minerals (Hacker *et al.* 2003). Kelemen *et al.* (2003) advocated an alternative interpretation whereby water-rich silicate melts from the subducted slab induce mantle melting. Subduction-derived fluids and melts rise into the base of the overlying mantle, corroding existing mantle minerals and forming new hydrous silicates. Hydrated mantle minerals release more water as induced convection drags these deeper. Released fluids percolate upwards into the hotter (asthenospheric) parts of the mantle wedge (Fig. 10), where they dramatically lower

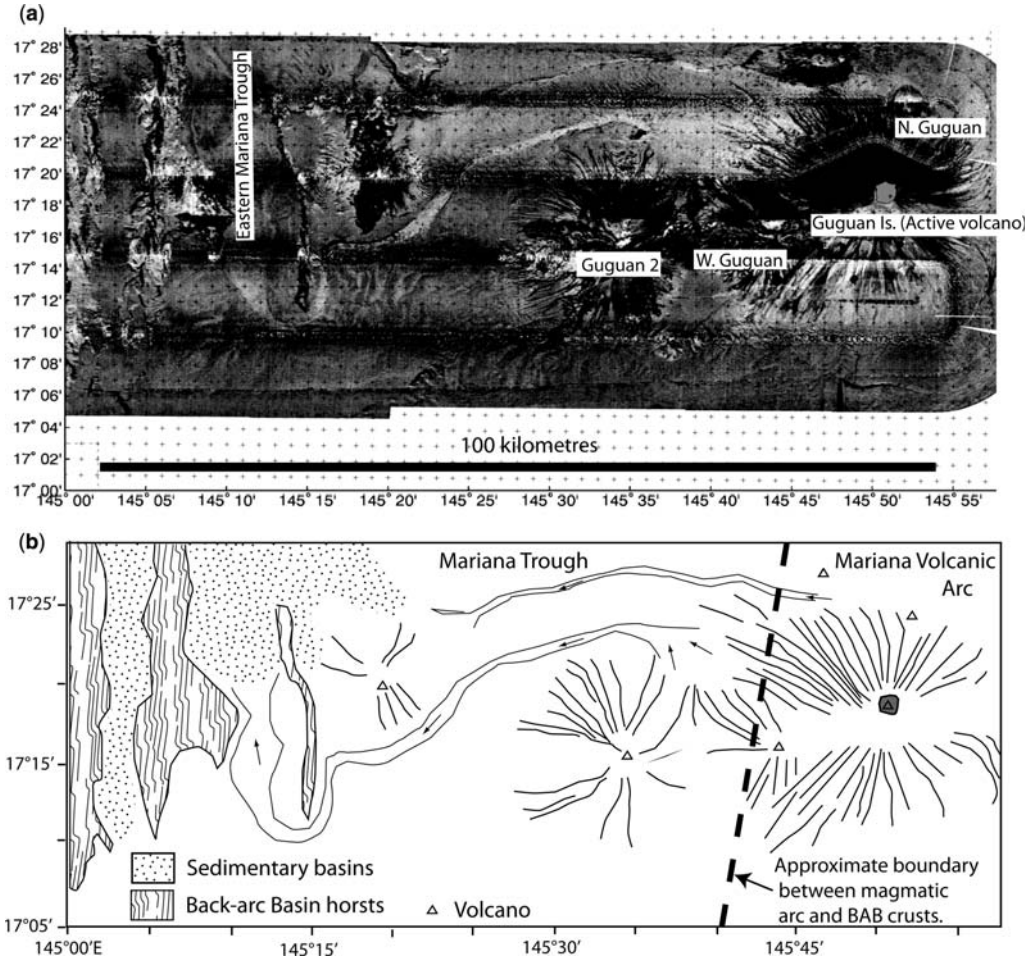

Fig. 9. Example of a large-scale sediment transport system associated with a mostly submarine IOAS. (**a**) HMR-1 sonar backscatter image of the Guguan cross-chain in the Mariana arc (Stern *et al.* 2006; location shown in Fig. 7). The volcanic–magmatic front is represented by Guguan island and submarine North Guguan volcanoes. The Guguan cross-chain extends due west from Guguan and trends perpendicular to the volcanic–magmatic front. The two long channels responsible for moving volcaniclastic sediments westward into deeper water on the eastern flank of the Mariana Trough BAB should be noted. (**b**) Interpretation sketch map of HMR-1 image in (a). See text for further discussion.

the temperature of peridotite and metasomatize the mantle source with fluid-mobile trace elements (K, Rb, U, Pb, etc.), giving the hybridized mantle source the distinctive trace element signature of arc melts, as discussed below. Melting as a result of decompression may also be important (Plank & Langmuir 1988; Conder *et al.* 2002).

The trenchward limit of asthenospheric flow in the core of the mantle wedge determines the location of the volcanic–magmatic front (Cagnioncle *et al.* 2007). Because fluid flux from the subducted slab decreases with increasing depth, the interaction of asthenosphere with the greatest fluid flux maximizes melt generation; because fluid flux diminishes with greater depth to the subducted slab and distance from the trench, melt generation also decreases rapidly in this direction. The characteristic depth to the subduction zone of *c.* 110 km below the volcanic–magmatic front probably reflects the minimum thickness of overriding crust and mantle that is required to allow asthenosphere to circulate.

Strong asymmetries are seen in IOAS magmatic products. Igneous activity in the forearc occurs only early in the life of an IOAS, as discussed below. Lavas erupted along the magmatic–volcanic front are dominated by tholeiitic and high-Al basalts and calc-alkaline andesites (and their differentiates;

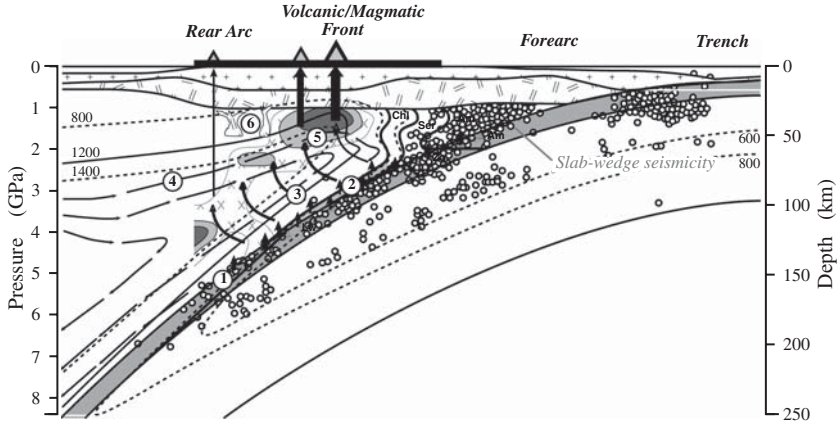

Fig. 10. Generation of melts in the mantle wedge beneath a convergent (intra-oceanic) margin, showing simplified processes modelled by Kimura & Stern (2008). 1, Dehydration and progressive metamorphism of subducted sediment, altered oceanic crust, and serpentinized lithosphere; 2, hydration–dehydration of mantle wedge sole and upward migration of supercritical hydrous fluid; 3, fluid transport and zone refining of mantle wedge; 4, induced asthenospheric convection; 5, open-system melting in the mantle wedge; 6, delamination of lower crust and refertilization of underlying asthenospheric mantle. This section is based on seismic tomography beneath NE Japan, Moho depth, crustal structure, and mantle wedge isotherms (dotted fine line with numbers; °C) and flow lines (fine black arrows). Hydrous mineral stability fields: Ser, serpentine; Am, amphibole; Zo, zoisite; Cld, chloritoid; Lw, lawsonite. Grey open circle, earthquake location; arrows indicate, from bottom to top, path of dehydrated fluid, first from subducted crust, sediments, and serpentinite; then from serpentinized wedge sole. Fluids traverse to the centre, hottest part of the mantle wedge, where shades and patterns map temperature and fluid or melt generation inferred from variations in V_s (Zhao *et al.* 1994). Vertical arrows from region of melt generation indicate basalt migration through crust to surface.

Kelemen *et al.* 2003). Rear-arc cross-chains are dominated by more enriched calc-alkaline and shoshonitic lavas. Back-arc basin basalts are tholeiitic, similar in most respects to MORB. These magmatic products are discussed in greater detail below.

Relative to other mantle-derived melts [MORB and ocean island basalt (OIB)], arc melts are enriched in silica, water, and large ion lithophile elements (LILE; e.g. K, U, Sr, and Pb). Figure 11 summarizes the distinctive trace element patterns of primitive (i.e. unfractionated) basalts from IOAS volcanic fronts. The trace element patterns observed for these lavas (and the derivatives of these melts, including fractionates and anatectic melts) show distinctive and similar trace element characteristics that testify to the processes shown in Figure 10, including high degrees of melting of hydrous metasomatized mantle in the spinel peridotite facies. First, the mantle melts more beneath a typical IOAS volcanic front than does the mantle associated with mid-ocean ridges or oceanic hotspots. This is shown by low Na_2O contents of primitive arc basalts (which vary inversely with extent of melting) and by low contents of incompatible trace elements that are not fluid-mobile [i.e. Ti, Zr, Nb, and heavy rare earth elements (HREE)]. For example, the dashed horizontal line approximates the abundances of fluid-immobile elements Zr to the HREE, which are *c.* 60% of those found in MORB. This implies that the mantle melts *c.* 70% more beneath IOAS volcanic fronts than it does

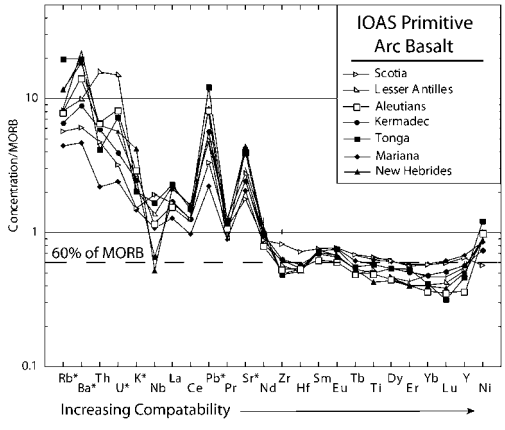

Fig. 11. Extended trace-element diagrams for average primitive IOAS active arc basalts. Concentrations are normalized to N-MORB (Hofmann 1988). Primitive arc basalts are remarkably similar, and consistently distinct from MORB. Elements with asterisks indicate fluid-mobile trace elements. Modified from Kelemen *et al.* (2003).

beneath mid-ocean ridges. Second, the greater melting beneath arcs reflects the important role that water plays in mantle melting and the much greater abundance of water in IOAS magmas relative to MORB or even hotspot basalts (Stern 2002). IOAS volcanic front lavas are typically coarsely porphyritic, consisting of phenocrysts of An-rich plagioclase and Fe-rich olivine (Fig. 12). This is best explained by high magmatic water contents suppressing the crystallization of plagioclase and rotating its solvus. IOAS volcanic front lavas are typically much more porphyritic than MORB or OIB, consistent with an interpretation that loss of magmatic water during ascent drove rapid crystallization. Third, elevated abundances of fluid-mobile elements such as LILE, shown as positive concentration spikes in Rb, Ba, U, K, Pb, and Sr (Fig. 11), are best explained as resulting from metasomatism of the mantle source region by hydrous fluids or melts. Finally, the flat HREE patterns shown by IOAS basalts are inconsistent with residual garnet in the mantle source region, instead suggesting melt generation in the spinel peridotite stability field. Spinel peridotite is stable at pressures corresponding to depths of 15–80 km, consistent with the expected position of the asthenosphere in the mantle wedge.

Primitive IOAS magma rises into the arc crust, where it may be temporarily stored in magma reservoirs, differentiate and mix with other magmas. The tremendous heat associated with the magmatic front also can lead to crustal anatexis and delamination to generate more felsic arc crust. The twin processes of magmatic fractionation and anatexis, responsible for producing IOAS felsic melts, occur in the crust.

To a certain extent, IOAS magmas reflect the arc's evolutionary stage as well as depth to the subducting slab. Early in the history of an IOAS, lavas are dominated by high-degree melts such as boninites and tholeiites (and their differentiates). It is not yet clear whether melts of the magmatic front evolve systematically as the arc ages. The Izu–Bonin–Mariana IOAS shows no systematic compositional evolution once the magmatic front stabilized *c.* 40 Ma ago (Straub 2003), whereas the Greater Antilles IOAS seems to have evolved from early tholeiites to later calc-alkaline and then shoshonitic lavas (Jolly *et al.* 2001). Systematic changes in melt composition may reflect changing upper plate stresses (lithospheric extension v. compression), or may be related to evolving crustal thickness (thicker crust encourages melt stagnation, enhancing fractionation and anatexis), or thermal conditioning (mature arcs with thick crust are

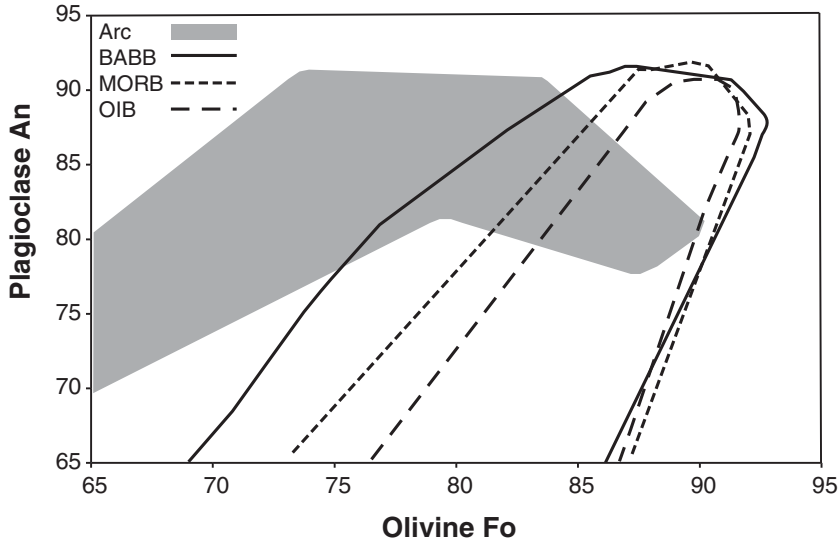

Fig. 12. Composition ranges for olivine–plagioclase assemblages for intra-oceanic arc and back-arc basin basalts (BABB) compared with those for OIB and MORB. Assemblages in basalts from the volcanic front show distinctively high-An (>85) feldspar in more evolved melts in equilibrium with Fo_{70-85} olivine. This is due to stabilization of high-An feldspar in hydrous melts. Anhydrous decompression melt assemblages show similar decreases in Plag An and Ol Fo with melt evolution. BABB assemblages are similar to those of MORB and OIB but partially overlap the arc range. Data for arc field compiled from Basaltic Volcanism Study Project (1981) and intra-oceanic arcs databases at PetDB; BABB from PetDB; MORB field from PetDB (Allan *et al.* 1987; Basaltic Volcanism Study Project 1981; Davis & Clague 1987); OIB field compiled from PetDB, Basaltic Volcanism Study Project (1981) and Garcia *et al.* (2000). Pairs of data points for fields: Arcs, 210; OIB, 178; MORB, 151; BABB, 112. Figure generated by E. Kohut.

more likely to experience anatexis around magmatic conduits and reservoirs). Systematic changes in the age of subducting lithosphere could also change IOAS active arc melt compositions, because subduction of very young (hot) oceanic crust (<20 Ma old) can melt to produce adakites (Defant & Drummond 1990). Because IOASs are concentrated where old, dense oceanic lithosphere is subducted, this mode of magmagenesis is not a significant aspect of modern IOASs.

IOAS igneous activity in mature systems is concentrated at the volcanic–magmatic front but can also occur farther away from the trench, along rear-arc or cross-chain volcanoes and in back-arc basins. These two magmatic regimes are very different. Rear-arc volcanoes are common in some IOASs such as the Izu, Bismarck, or Kurile arcs but not in others such as Tonga–Kermadec. Where cross-chains occur they comprise a few to several smaller volcanoes that extend away from a large volcanic front edifice at high angles. Rear-arc volcanoes erupt lavas that are more primitive (Mg-number >60) than volcanic front lavas. These rear-arc lavas are also less porphyritic and do not show the plagioclase–olivine compositional relationships characteristic of IOAS volcanic front lavas. These characteristics, along with the generally more enriched nature of cross-chain lavas, reflect diminished extent of melting as a result of lower fluid flux from the slab with greater distance from the trench. This is the basis for the K–h relationship, which describes the relative enrichment in K and other incompatible elements in arc lavas as a function of depth to the underlying subduction zone (Dickinson 1975; Kimura & Stern 2008).

The final locus of IOAS igneous activity occurs in BABs. Back-arc basin magmas are dominated by tholeiitic basalts that range from MORB-like to arc-like (Pearce & Stern 2006). BAB basalt (BABB) magmas are typically more hydrous than MORB (1–2% v. <0.5% water; Stern 2002). Compositions of BABBs result from four factors: (1) the composition of asthenosphere flowing into the region of melting beneath the BAB spreading ridge; (2) the composition and relative impact of a fluid- or melt-dominated subduction component; (3) how asthenosphere and subduction components interact; (4) the melting of water-rich mantle and the assimilation–crystallization history of the resulting hydrous magma. Trace element and water contents of BAB glasses indicate that decompression melting (similar to that beneath mid-ocean ridges) beneath back-arc basins is augmented by flux melting as a result of the abundance of hydrous fluids.

BAB spreading is generally asymmetric, with spreading axes often lying closer to the active volcanic arc than the remnant arc. BABs have relatively short lifespans compared with volcanic arcs, up to a few tens of million years. This is because as a BAB matures and widens the neovolcanic zone increases in distance from the trench, so that the water flux into the melting region decreases with time. Correspondingly, magma production diminishes over a BAB's life. Such a progression is observed for the 30–15 Ma old Parece Vela Basin, which progressed from magmatic spreading to amagmatic rifting before spreading stopped completely (Ohara 2006). These controls on melting and extension lead to the cessation of BAB spreading after a few tens of million years.

Because BAB basalts and gabbros have compositions and crustal structures that are similar to those of typical oceanic crust, but with trace element enrichments only found in convergent margins, they are often thought to be where ophiolites with 'supra-subduction zone' (SSZ) compositions form (Dilek 2003; Pearce 2003). Some ophiolites may originate in back-arc basins but most probably form in forearcs, where they are in a tectonic position that is much more likely to be emplaced on top of buoyant crust (obducted) if and when this arrives at a subduction zone (Stern 2004). The presence of boninites, which are common in forearcs but rare in BABs, may help resolve such uncertainty, but boninites are found only in some forearcs. Correspondingly, the absence of boninites in an SSZ ophiolite should not be taken as necessarily indicating that the ophiolite formed in a BAB instead of a forearc. Another way to distinguish BAB from forearc crust is that BAB crust forms at intervals after the magmatic arc, whereas forearc crust forms before the magmatic arc.

The nature of IOAS lower crust and upper mantle

The 'classic' Moho is strictly defined on the basis of seismic velocities to separate crust (V_p *c.* 6–7 km s^{-1}) from upper mantle ($V_p > 8$ km s^{-1}). This generalization does not hold for IOASs, where such Moho is rare beneath the forearcs and magmatic front, although the sub-BAB Moho is clear. The variable expression of Moho beneath IOAS magmatic front, forearc, and back-arc basins reflects different compositions and alteration histories. Simply put, forearc peridotites are dominated by harzburgite (Parkinson & Pearce 1998; Pearce *et al.* 2000) and are most serpentinized; peridotites associated with the active magmatic arc contain abundant pyroxenite and pyroxene-rich lithologies in addition to lherzolite and harzburgite; and back-arc basin peridotites are mostly lherzolites, similar

in most regards to those associated with slow-spreading mid-ocean ridges.

Because the BAB Moho is the best defined, we discuss the composition of the upper mantle below this first. Until recently we had no samples of BAB peridotite to study but we now have had a chance to study peridotites from the northern Mariana Trough (Ohara *et al.* 2002) and the Parece Vela Basin (Ohara 2006). The Parece Vela Basin formed in Miocene time by fast to intermediate rates of sea-floor spreading and includes residual lherzolite and harzburgite, along with plagioclase-bearing harzburgite and dunite. These peridotites are similar to those of the Romanche Fracture Zone in the Mid-Atlantic Ridge and Indian and Arctic Ocean slow-spreading ridges. In contrast, the Mariana Trough is a typical slow-spreading ridge and it locally yields residual harzburgite that is also similar to that recovered from slow-spreading mid-ocean ridges. These two examples of BAB peridotites reveal different melt–periodite interactions. The Parece Vela peridotites were affected by diffuse porous melt flow and pervasive melt–mantle interaction. Abundant dunites represent melt conduits, where melt and pyroxene reacted to form olivine. In contrast, the Mariana Trough peridotites are characterized by channelled melt–fluid flow and limited melt–mantle interaction.

Forearc peridotites (recovered from inner trench walls) are mostly harzburgites that are more depleted than abyssal peridotites from mid-ocean ridges. Forearc peridotites generally are the most depleted peridotites that form on Earth today (Bonatti & Michael 1989). This is shown by their low Al_2O_3 and elevated SiO_2, reflecting the fact that these are more orthopyroxene-rich than residues of fertile mantle peridotite (Herzburg 2004). Herzburg (2004) suggested on this basis that they were produced by melt–rock reaction. The extreme depletion of forearc peridotites is also shown by the composition of their spinels. Spinel is sensitive to melt depletion, which is reflected in $Cr/(Cr + Al)$. Spinel is also very resistant to alteration and generally preserves petrogenetic information in spite of significant serpentinization (Dick & Bullen 1984). Forearc peridotites have high-Cr-number ($Cr/(Cr + Al) > 0.4$) spinel. These forearc peridotites are variably serpentinized, being more altered near the trench, and less altered towards the magmatic front. Serpentinization makes seismic recognition of the Moho difficult.

Multiple perspectives are needed to understand the mantle beneath IOAS magmatic arcs. One perspective comes from rare mantle xenoliths brought up in arc lavas. Arai & Ishimaru (2008) summarized this for West Pacific arc lavas. These are mostly from arcs built on continental crust but still provide an important glimpse of the mantle beneath the magmatic front. Almost all the peridotite xenoliths are spinel-bearing varieties without garnet or plagioclase. Arai & Ishimaru (2008) emphasized that mantle metasomatism is most pervasive and long-lived beneath the volcanic front, where magma transit is very long-lived. Metasomatism here reflects the importance of silica-rich, hydrous melts, and is likely to be manifested in the formation of secondary orthopyroxene at the expense of olivine. A large range of fertility and depletion is seen in arc xenoliths. Some are more fertile than the most fertile abyssal lherzolites, whereas others are more depleted than the most depleted abyssal peridotite. This lithological variation is probably due to the complex tectonic history of each as well as to across-arc variation in magma production conditions.

A second useful insight into the nature of the lower crust and upper mantle beneath the magmatic front comes from active source geophysical soundings of IOASs; investigations of the central Aleutian IOAS are particularly useful. Fliedner & Klemperer (2000) interpreted these results to indicate *c.* 30 km thick crust underlain by heterogeneous uppermost mantle ($V_p = 7.6–8.2$ km s^{-1}). Shillington *et al.* (2004) reinterpreted the same dataset to indicate that the crust was 20% thicker than concluded from the earlier study. They interpreted the regions with velocities of 7.3–7.7 km s^{-1} as lower crust made up of ultramafic–mafic cumulates and/or garnet granulites. They also found upper mantle velocities of 7.8–8.1 km s^{-1} at greater depth, significantly higher than that inferred from the Fliedner & Klemperer study. A similar situation is seen for the Izu–Bonin–Mariana IOAS. High-resolution seismic profiling (Kodaira *et al.* 2007; Takahashi *et al.* 2007) reveals an unusually low-velocity (7.2–7.6 km s^{-1}) material in the lower crust–upper mantle transition zone. This is interpreted at present as an uppermost mantle layer between the Moho above and reflectors in the upper mantle below. These velocities are best explained by a broad crust–mantle transition zone that is rich in pyroxene and/or amphibole.

P-wave velocity structure of the Mariana IOAS and complementary interpretation is shown in Figure 13 (Takahashi *et al.* 2008). Takahashi *et al.* (2008) found that the P-wave mantle velocity beneath the magmatic front is 7.7 km s^{-1}, markedly less than the normal upper mantle V_p of 8.0 km s^{-1}. Based on its continuity, Takahashi *et al.* (2008) identified the base of the 6.7–7.3 km s^{-1} layer as Moho. It should be noted that the sub-Moho reflectors lie beneath the Mariana arc magmatic front, the West Mariana Ridge (remnant arc), and the Mariana Trough spreading axis, in a part of the mantle that is characterized by low V_p (<8 km s^{-1}). These reflections might indicate rising magma bodies in the

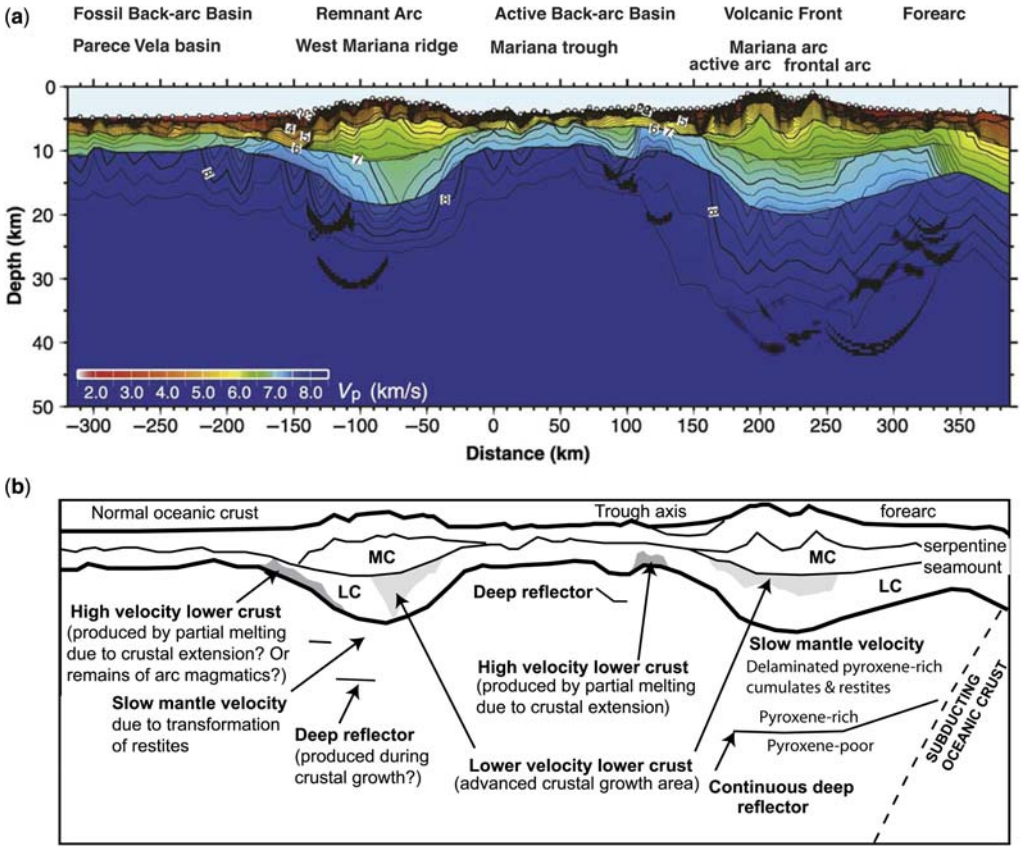

Fig. 13. (**a**) Velocity structure of the Mariana Arc (see Fig. 7 for location of profile; from Takahashi *et al*. (2008). Numerals indicate P-wave velocity (km s^{-1}). Thick black lines in blue area (inferred mantle) indicate positions of deep reflectors, perhaps marking boundaries in uppermost mantle separating upper regions with abundant pyroxene and pyroxenite from those below dominated by peridotite. (**b**) Schematic interpretation of seismic profile in (a) (modified after Takahashi *et al.* 2008).

upper mantle, or ghosts of dense lower crust that has sunk back into the mantle. The slow mantle region does not extend down to the upper mantle reflector. The 8.0 km s^{-1} velocity contour lies between the Moho and the deep reflector, which Takahashi *et al.* (2008) inferred has a velocity contrast of about 0.7 km s^{-1}. These observations are consistent with an interpretation that mantle peridotite dominates beneath the arc at depths >40 km, but the shallower mantle contains a significant proportion of pyroxenite and/or amphibolite.

The velocity structure of the Mariana IOAS is similar to that of other IOASs, at least those that have been studied in similar detail. Figure 14 compiles the P-wave velocity structure for 10 sites of three IOASs. These velocity profiles are beneath the active arc, except for one profile beneath the Mariana forearc. Comparison of the velocity structure beneath the Mariana active arc–forearc pair suggests that the forearc structure is *c.* 0.25–0.5 km s^{-1} slower than the active arc, but it is not yet known whether this is a systematic difference between forearc and active arc crustal structure. Most of the profiles show increases to V_p *c.* 7.8 km s^{-1} or more, interpreted to correspond to upper mantle and thus marking the Moho, at depths between 25 and 35 km. This is where IOASs are thickest, but is nevertheless significantly thinner than continental crust, which is typically *c.* 40 km thick. IOAS crust also differs from continental crust in being significantly faster (by 0.5–1.0 km s^{-1}) than typical continental crust. This indicates that IOAS crust is more mafic than continental crust.

A complementary perspective comes from fossil arcs in orogens, where deep crust and upper mantle

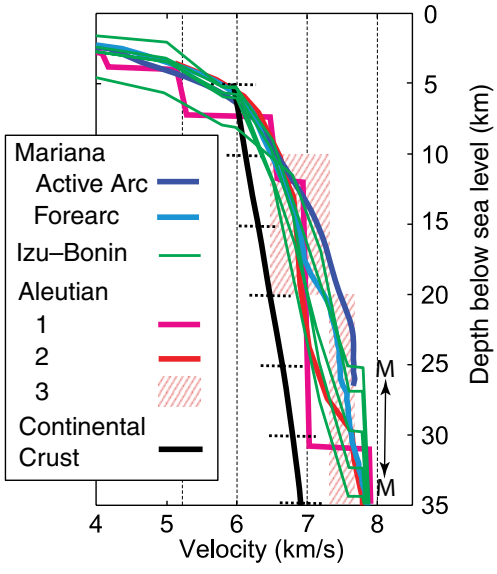

Fig. 14. Comparison of average P-wave velocities at 10 sites from three intra-oceanic arcs (Mariana, Izu–Bonin, and Aleutian), modified after Calvert *et al.* (2008). Profiles for Mariana are from Calvert *et al.* (2008); for Aleutian 1 after Holbrook *et al.* (1999); Aleutian 2 after Fliedner & Klemperer (2000); Aleutian 3 after Shillington *et al.* (2004); and five Izu–Bonin arc profiles are from Kodaira *et al.* (2007, fig. 8) at 162, 260, 307, 365, and 435 km. M, depth range of Moho. A noteworthy feature is the broad similarity of the 10 profiles, all of which are significantly faster (by 0.5–1.0 km s^{-1}) than typical continental crust (shown with 1 standard deviation, from Christiensen & Mooney 1995). All profiles are beneath active arcs except Mariana forearc, where upper crustal P-wave velocities are 240–360 m s^{-1} slower than beneath the active Mariana arc at equivalent depths.

are often exposed. The best studied examples are Mesozoic IOASs of Talkeetna (Alaska) and Kohistan (Pakistan). Reconstruction of the fossil (Jurassic) Talkeetna arc by Hacker *et al.* (2008) indicated *c.* 35 km crustal thickness. Hacker *et al.* (2008) reconstructed the following major layers, from top to bottom (Fig. 15): (1) a *c.* 7 km thick volcanic section (Clift *et al.* 2005); (2) intermediate plutonic rocks (tonalites and quartz diorites) at 5–12 km depth; (3) mafic metamorphosed gabbroic rocks from 12 to 35 km depth. These metagabbroic rocks include: (1) hornblende gabbronorites down to *c.* 25 km; (2) garnet diorites, first appearing at *c.* 25 km depth; (3) garnet gabbro, spinel-rich pyroxenite and orthogneiss, and hornblende gabbronorite at the base of the arc at *c.* 30–35 km depth (Fig. 15). The upper mantle beneath Talkeetna consists of abundant pyroxenites, consistent with inferences from geophysical studies of the Aleutians and Izu–Bonin–Mariana IOASs. The abundance of pyroxenite in the upper mantle beneath the active magmatic arc contrasts markedly with the more depleted, harzburgitic mantle beneath the forearc. The Border Ranges ultramafic complex fragments in the McHugh mélange complex were suggested by Kusky *et al.* (2007) to be the ophiolitic forearc to the Talkeetna IOAS

The upper mantle beneath the Cretaceous Kohistan palaeo-arc also contains abundant dunite, wehrlite, and Cr-rich pyroxenite in the inferred Moho transition zone [Jijal complex; (Garrido *et al.* 2006)]. Dhuime *et al.* (2007) reported that dunites, wehrlites and pyroxenites make up *c.* 50% of the Jijal complex. The origin of sub-arc pyroxenites and their relationship with the surrounding gabbros is controversial here as well. Are they cumulates from the fractionation of mafic magmas or do they result from melt– or fluid–rock interaction in the upper mantle? It is likely that sub-arc pyroxenites have multiple origins, some forming by reaction within the upper mantle, others forming in the lower crust and sinking back into the mantle as a result of delamination.

A key consideration for understanding how the lower crust and upper mantle beneath active magmatic arcs developed and behaves comes from advances in understanding the thermal structure of IOASs. Temperatures in IOAS lower crust, near the Moho beneath active magmatic arcs, approach or exceed 1000 °C. Because active arc volcanoes mark the surface projection of magma transport routes at depth, Moho temperatures probably also vary along strike of the arc, being higher beneath volcanoes and lower between them. In addition, temperatures in the crust beneath IOAS volcanic arcs may not vary smoothly with depth, but are strongly controlled by rheology. Figure 16b summarizes the rheological control on arc thermal structure, showing that a significantly lower thermal gradient exists through the upper, brittle part of the crust, where seawater is able to circulate through fractures and faults. At a certain depth in the middle crust corresponding to the brittle–ductile transition, such fractures and faults are annealed and a step in the geothermal gradient is likely to result from advective ascent and ponding of magmas. Regardless of this step in the geothermal gradient, temperatures of 800–1200 °C have been determined and inferred for IOAS Moho. Such a thermal structure implies significant remelting of mafic arc crust roots, depending on the composition of lower IOAS crust. If it is dry (meta-mafic granulite), solidus temperatures lie well below likely IOAS geotherms and remelting of IOAS arc crust is unlikely (Fig. 16c). On the other hand, if amphibole is an important component of IOAS arc crust, then the solidus should be significantly

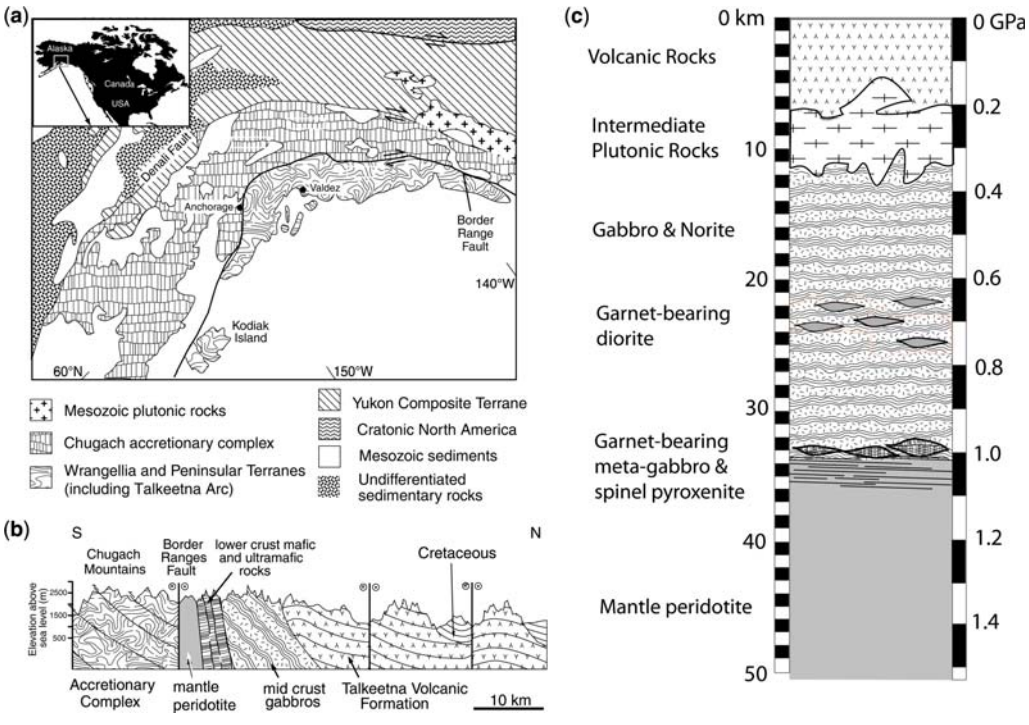

Fig. 15. (**a**) Tectonic map of Alaska and NW Canada showing the location of the Talkeetna arc and other exotic terranes accreted to cratonic North America. The study region is located within the Peninsular Terrane of south–central Alaska, sandwiched between Wrangellia to the north and the Cretaceous accretionary complexes exposed within the Chugach Terrane to the south (modified after Clift *et al.* 2005). Terrane boundaries are all faulted. The Talkeetna arc sequence is also associated with a fragmented forearc basement, a few million years older than the arc sequence (Kusky *et al.* 2007). (**b**) Schematic cross-section through the Talkeetna arc, showing the general northward dip of the arc, dissected by east–west strike-slip faults (modified after Clift *et al.* 2005). (**c**) Pseudostratigraphic column for the Talkeetna arc, modified after reconstruction of Hacker *et al.* (2008). K-feldspar-bearing plutons crystallized at 5–9 km, most hornblende gabbronorites crystallized at 17–24 km, garnet-bearing diorites crystallized at 22–24 km, and garnet gabbros crystallized at the base of the arc at *c.* 30 km depth.

lower than the geotherm (Fig. 16d) and remelting of large parts of the lower crust seems inevitable. Fractional crystallization coupled with anatexis in the lower arc crust seems likely, and dense residues and fractionates are likely to sink back into the upper mantle. In support of this idea, Brophy (2008) concluded from consideration of REE modelling that felsic magmas in IOASs could be produced either by fractional crystallization (with or without hornblende) or by amphibolite melting, and that fractional crystallization seemed to be the dominant mechanism.

The Talkeetna fossil arc again provides important insights into the fate of lower crust beneath IOAS magmatic fronts. Field studies show that the great volumes of mafic and ultramafic cumulates (gabbronorite and pyroxenite) expected to have been produced by fractionation of primitive, mantle-derived melts are missing from the lower crust. Behn & Kelemen (2006) argued that lower crustal $V_p > 7.4$ km s^{-1} in modern arcs indicates material that is gravitationally unstable relative to underlying asthenosphere; such material is likely to sink into the mantle. They also noted that the lower crust beneath modern arc magmatic fronts has $V_p < 7.4$ km s^{-1}, indicating that pyroxene-rich lower crust is generally not present. These observations support the conclusion that large volumes of lower arc crust founder rapidly on geological time scales, or that a significant proportion of high-V_p cumulates form beneath the Moho (Behn & Kelemen 2006).

Based on petrological modelling and V_p estimates for sub-Izu–Bonin–Mariana crust and mantle, Tatsumi *et al.* (2008) inferred that the uppermost mantle low-V_p layer was composed of mafic,

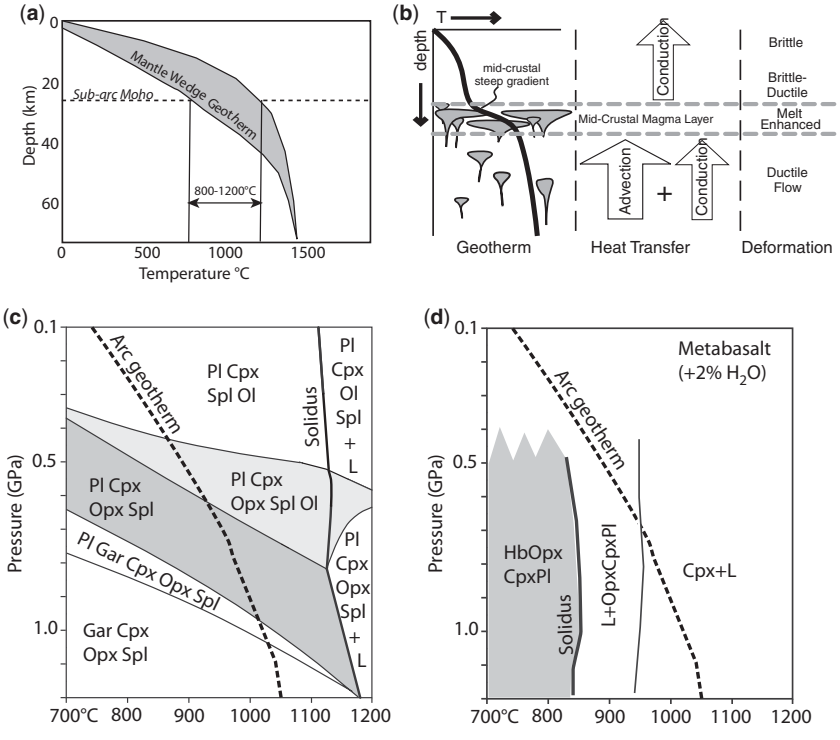

Fig. 16. Thermal structure of IOAS beneath volcanic–magmatic front. (**a**) Geothermal gradient in crust and mantle beneath the active volcanic–magmatic arc, simplified after Hacker *et al.* (2008). Mantle beneath the Moho of active magmatic arc is at 800–1200 °C and therefore will be weak. Dense, delaminated lower crustal materials could easily sink into this buoyant, weak mantle. (**b**) Schematic illustration of how a magma-rich layer could produce steep geothermal gradients in the middle crust. Advective heat transport below the level of magma emplacement is more efficient than conductive transport above. This forces steep geothermal gradients to form in the middle crust, separating low-temperature upper crust from higher temperature lower crust. Deformation below the magma layer is by penetrative ductile flow; deformation above the layer is focused in narrow shear zones (Shaw *et al.* 2005). (**c**) Phase relations for Talkeetna orthogneiss 1709P11, showing pressure-induced consumption of olivine from the igneous assemblage feldspar (fsp) + clinopyroxene (cpx) + orthopyroxene (opx) + spinel (spl) + olivine (ol) ± liquid (L) to produce cpx + opx + spl symplectite. A range of P–T paths compatible with this inferred transformation is shown (Hacker *et al.* 2008). (**d**) Simplified phase relationships for the hydrous synthetic low-K basalt with 2 wt% H_2O added compositions (Nakajima & Arima 1998). Solidus for anhydrous compositions is at *c.* 1150 °C, significantly hotter than typical arc crustal geotherm, but solidus for hydrous compositions is at *c.* 850 °C, well below the arc geotherm.

pyroxene-rich material that had sunk back into the mantle, not mantle peridotite. It appears that igneous activity beneath IOAS active magmatic arc evolves from mafic to intermediate as a result of continuous loss of mafic and ultramafic lower crustal components to the subarc mantle across a chemically transparent Moho (Tatsumi *et al.* 2008). This process will slow crustal thickening at the same time that increasingly felsic crust comes to make up the evolving arc crust, leading to a crustal thickening rate of *c.* 500 m Ma^{-1}. When IOAS crust thickens sufficiently to stabilize garnet in the lower crust (greater than *c.* 30 km thick), magma compositions will become more adakitic at the same time that delamination and crustal processing are likely to be enhanced [as a result of the greater density of garnet (3.6 g cm^{-3}) relative to pyroxene (3.2 g cm^{-3})]. This model is summarized in Figure 17.

IOAS forearc structure preserves early history

A final important point about IOASs concerns how they form, how the forearc is built and abandoned as a site of igneous activity, and how the active magmatic arc finally comes to the position that it subsequently occupies for as long as the IOAS exists. IOASs begin their evolution when subduction

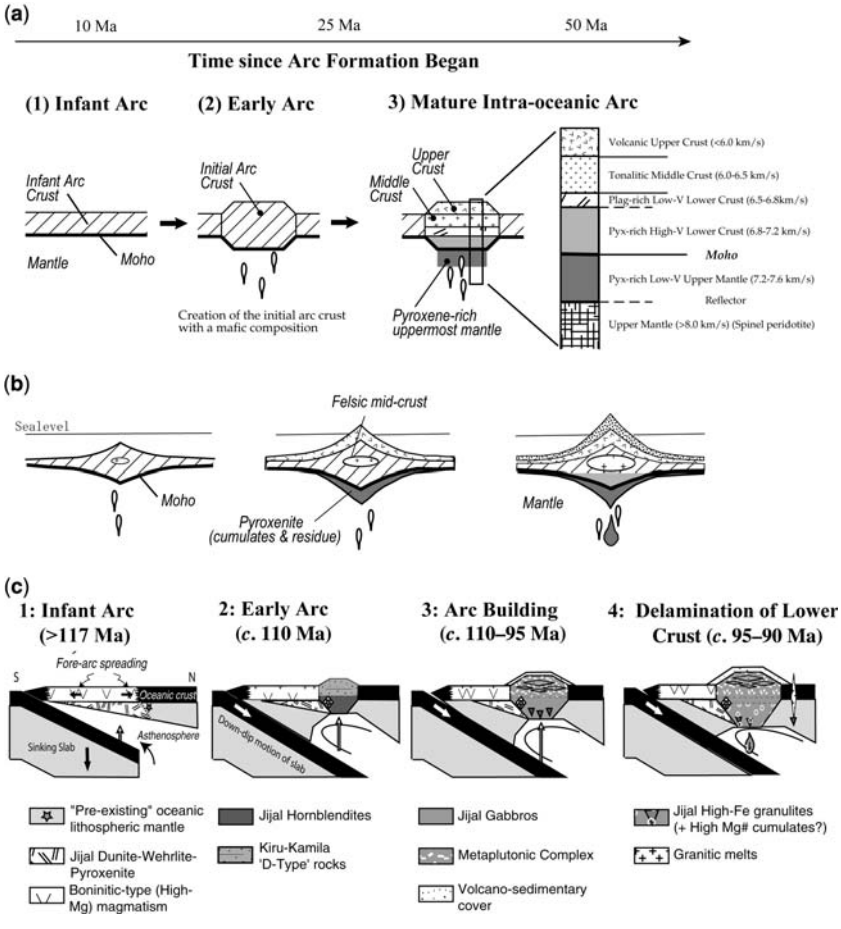

Fig. 17. Formation and refinement of juvenile arc crust. (**a**) Model of arc crust evolution from Tatsumi *et al.* (2008). (1) Incipient arc magmatism replaces the pre-existing oceanic crust to create (2) the initial mafic arc crust. (3) Continuing arc magmatism causes anatexis and differentiation of the arc crust, along with transformation of mafic crustal component into the mantle through the Moho, finally creating mature arc crust with an intermediate composition similar to the average continental crus. Generalized seismic velocity structure in the IBM arc after Suyehiro *et al.* (1996), Kodaira *et al.* (2007) and Takahashi *et al.* (2007). (**b**) Schematic illustration of progressive burial of early formed plutonic and volcanic rocks within a growing arc (modified after Kelemen *et al.* 2003). Pyroxenites near the base of the crust are denser than the underlying mantle, and temperatures are high near the Moho, so that these ultramafic cumulates may delaminate whenever their thickness exceeds some critical value (e.g. Jull & Kelemen 2001). Increasing pressure forms abundant garnet in Al-rich gabbroic rocks near the base of the section, and these too may delaminate. Intermediate to felsic plutonic rocks, and even volcanic rocks, may be buried to lower crustal depths, where they are partially melted. (**c**) Four-stage schematic evolution of the Kohistan arc during the period 117–90 Ma (after Dhiume *et al.* 2007). Four evolutionary stages span the history of the arc, from spontaneous initiation of subduction associated with extensive boninitic magmatism (stage 1) to arc building by tholeiitic basalts (stages 2 and 3) and a fourth stage of intracrustal differentiation. Stage 4 culminated in the intrusion of granitic rocks akin to continental crust in the upper level of the metaplutonic complex.

begins. Subduction zones can form either as a result of lithospheric collapse (spontaneous nucleation of subduction zone; SNSZ) or by forced convergence (induced nucleation of subduction zone; INSZ; Stern 2004). For SNSZ, IOASs start as broad zones of sea-floor spreading associated with subsidence of the adjacent lithosphere, whereas INSZ IOASs may be built on trapped crust, without construction of new arc substrate by large-scale sea-floor spreading. SNSZ results from gravitational instability of oceanic lithosphere adjacent to lithospheric zones of weakness such as fracture

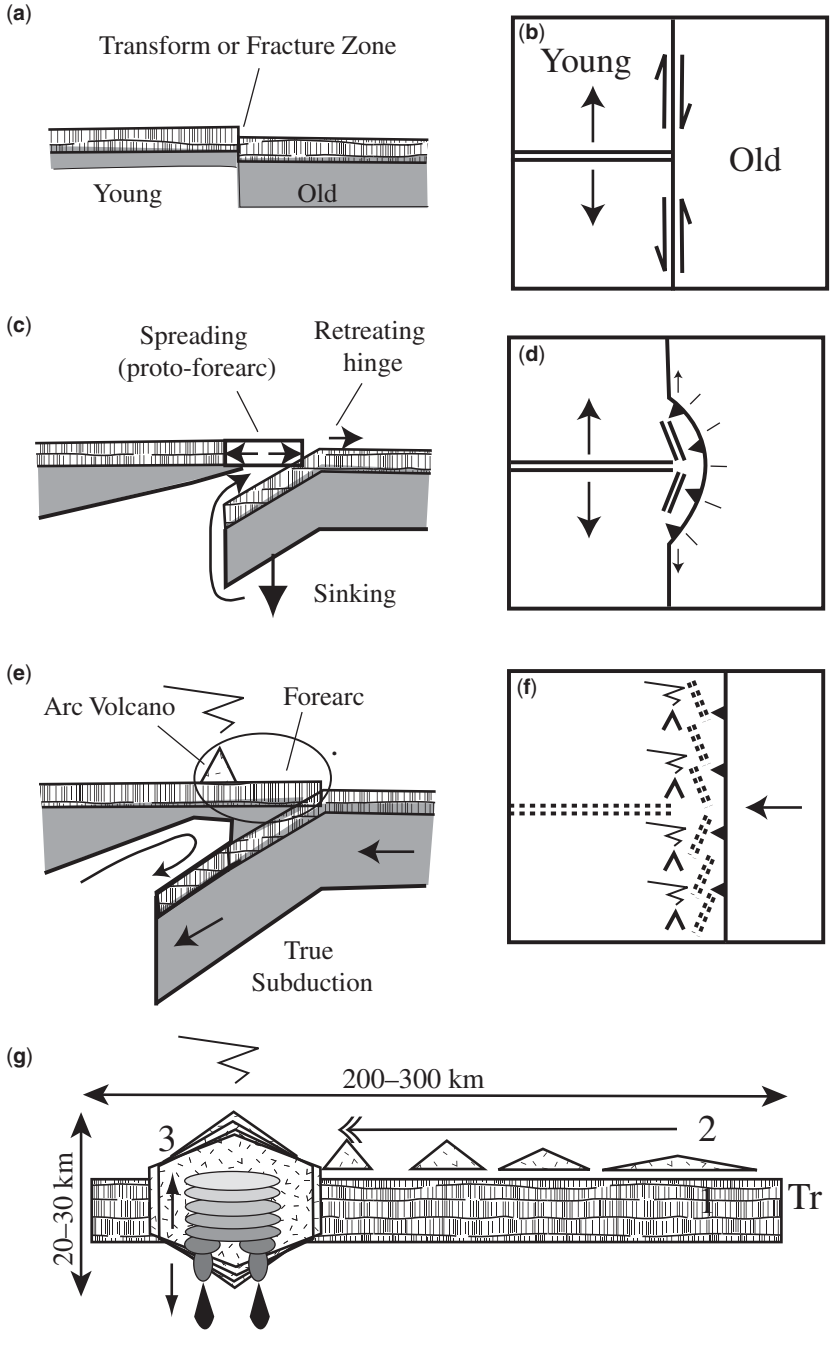

Fig. 18. Generation of forearc during subduction initiation and retreat of magmatic arc to the approximate position that it will subsequently occupy. (a–e) Subduction infancy model of Stern & Bloomer (1992), modified to show the third dimension. Left panels are sections perpendicular to the plate boundary (parallel to spreading ridge) and right panels are map views. (**a**, **b**) Initial configuration. Two lithospheres of differing density are juxtaposed across a transform fault or fracture zone. (**c**, **d**) Old, dense lithosphere sinks asymmetrically, with maximum subsidence nearest fault. Asthenosphere migrates over the sinking lithosphere and propagates in directions that are both orthogonal to the original trend of the transform or fracture zone as well as in both directions parallel to it. Strong extension in the region above the sinking lithosphere is accommodated by sea-floor spreading, forming infant arc crust of the proto-forearc.

zones (Fig. 18a, b). Because modern IOASs are concentrated in regions where the oceanic lithosphere is ancient, dense, and prone to collapse, it is likely that most IOASs form by SNSZ.

Lithospheric collapse to initiate SNSZ allows lighter asthenosphere to exchange places with denser, sinking lithosphere (Fig. 18c, d). This results in sea-floor spreading above the sinking lithosphere, and the combined result of decompression of rising asthenosphere and fluids released from the sinking slab is unusually high degrees of mantle melting. This produces very depleted tholeiites (low TiO_2 and K_2O) and subordinate boninites that make up the forearc crust. Felsic magmas are also produced during this 'infant arc' stage. Oceanic crust made up of these lavas and intrusions is underlain by genetically related ultradepleted harzburgitic mantle residues, and these rocks form what becomes the forearc. It is important to note that sea-floor spreading to form the forearc lasts only a few million years, while the subjacent lithosphere continues to sink and asthenospheric mantle flows above the sinking slab. This is the origin of most boninites and ophiolites. Stern & Bloomer (1992) argued that the Izu–Bonin–Mariana intra-oceanic arc system in the Western Pacific formed by collapse of old Pacific lithosphere east of a major transform, with much younger sea floor and hotter shallow mantle to the west. Stern & Bloomer (1992) estimated that during the first 10 Ma in the life of the Izu–Bonin–Mariana arc, melt generation occurred at a rate of *c.* 120–180 $km^3\ km^{-1}\ Ma^{-1}$. This may be a significant underestimate, because recent geophysical studies of the Izu–Bonin–Mariana and Aleutian arcs infer a mean crustal growth rate of *c.* 100 $km^3\ km^{-1}\ Ma^{-1}$ or more (Dimalanta *et al.* 2002; Jicha *et al.* 2006), orders of magnitude larger than mature arc eruption rates of $<10\ km^3\ km^{-1}\ Ma^{-1}$ (Kimura & Yoshida 2006; Carr *et al.* 2007).

Once down-dip motion of the slab (true subduction) begins, the asthenosphere is no longer able to flow into this region and the sub-forearc mantle rapidly cools. Slab-derived fluids migrating into the sub-forearc mantle no longer cause melting, only serpentinization. Igneous activity migrates away from the trench and eventually forearc igneous activity stops (Fig. 18e, f). A typical IOAS begins to mature when true subduction (i.e. down-dip motion of the sinking slab) begins and the subducted slab reaches *c.* 130 km depth, focusing magmatism to begin building the magmatic arc and allowing the forearc lithosphere to cool and hydrate. The zone of infant arc crust produced by sea-floor spreading above the subsiding lithosphere becomes forearc as the IOAS matures and the locus of magmatism retreats from the trench. This makes up the forearc, lithosphere that is emplaced as an ophiolite when buoyant lithosphere is subducted beneath it (Pearce 2003). Thus the forearc preserves the early history of the arc.

Intra-oceanic arc systems and the growth of the continental crust

In contrast to continuing controversy about how the modern inventory of continental crust came to be and what it was in the past (Dewey & Windley 1981; Armstrong 1991; Windley 1993), a broad geoscientific consensus exists that continental crust today is mostly generated above subduction zones, with secondary sites associated with rifts, hotspot volcanism, and volcanic rifted margins. Subduction zones are also the most important sites of crust removal, by sediment subduction, subduction erosion, and deep subduction of continental crust. A comprehensive overview of how continental crust is created and destroyed by plate-tectonic processes has been given by Stern & Scholl (2010).

Continental crust mostly forms today and over the lifetime that plate tectonics has operated by magmatic additions from water-induced melting of mantle above subduction zones (Coats 1962; Dimalanta *et al.* 2002; Davidson & Arculus 2005). This produces juvenile IOAS arc crust, and magmatically adds to pre-existing continental crust at Andean-type arcs. Scholl & von Huene (2009) estimated that over the last tens to hundreds of million years, *c.* 2.7 km^3 of juvenile continental crust has been generated by convergent margin igneous activity each year. This crust is mostly extracted from the mantle as mafic (basaltic or boninitic) magma, which must be further refined by anatectic remelting of the crust and delamination (foundering) to yield andesitic material approximating the

Fig. 18. (*Continued*) (**e**, **f**) Beginning of down-dip component motion in sinking lithosphere marks the beginning of true subduction. Strong extension above the sunken lithosphere ends, which also stops the advection of asthenosphere into this region, allowing it to cool and become forearc lithosphere. The locus of igneous activity retreats to the region where asthenospheric advection continues, forming a magmatic arc. (**g**) A detailed view of how magmatism in the arc evolves with time; 1, infant arc crust of the forearc ophiolite forms by sea-floor spreading during first *c.* 5 Ma of subduction zone evolution, as shown in (c) and (d); 2, retreat of magmatic activity away from the trench (Tr) during the second *c.* 5 Ma; 3, focusing of magmatic activity at the position of the active magmatic arc, resulting in crustal thickening and delamination.

bulk composition of continental crust (Rudnick & Gao 2003; Tatsumi 2005; Tatsumi *et al.* 2008). Although juvenile continental crust is mafic when first formed, it inherits from subduction zone processes the distinctive geochemical characteristics of subduction-related magmas: enrichment in silica and LILE (e.g. K, U, Sr and Pb) and depletion of high field strength incompatible elements (e.g. Nb, Ta and Ti). The similarity of trace element variations in arc rocks to that of bulk continental crust strengthens the inference that subduction-related magmatism is an impoirtant way to make continental crust today (Kelemen 1995; Rudnick & Gao 2003).

The distinctive chemical characteristics of IOAS magmas (Fig. 11) are likely to persist through later processing by anatexis within the crust and foundering of its base, so that juvenile mafic crust slowly matures into continental crust with andesitic bulk composition. The formation of continental crust at IOASs requires two stages: mantle melting to generate basalt and mafic crust and further refinement of this to yield granitic crust and refractory material, much of which founders back into the mantle (Hawkesworth & Kemp 2006). This is accomplished by distilling felsic magmas from mantle-derived juvenile crust via anatexis of amphibolites and fractional crystallization of mafic magmas. Much basaltic magma crystallizes as pyroxene-rich material near the Moho. Magmatic maturation of IOASs is also likely to occur in tandem with terrane accretion, whereby various juvenile crustal fragments coalesce to build progressively larger tracts of increasingly differentiated crust.

Conclusions

Intra-oceanic arc systems are enormous tracts of proto-continental crust, hundreds to thousands of kilometres long, several hundred kilometres wide, and up to 35 km thick. They tend to form where very old (>100 Ma) oceanic lithosphere is subducted, typically showing strong evidence for extension (normal faulting, intra-arc rifts, back-arc basins). Morphological asymmetries (trench, forearc, volcanic front, rear-arc volcanoes, and back-arc basin) reflect asymmetrical processes controlled by the dipping subduction zone. Crustal structure reflects this asymmetry, with IOAS crust thickening from the trench towards the magmatic front, and thinning again beneath back-arc basins. Distinctive compositions of igneous rocks and associated mantle also reflect the subduction-imposed asymmetries that reflect in part the evolution of the IOAS. Igneous rock compositions reflect decreasing water flux from the slab with distance from the trench, resulting in lower-degree melts and more enriched igneous rocks with this distance. This is the basis of the K–h relationship. In addition, ultrahigh-degree melting occurs early in the history of the IOAS to yield ultra-depleted tholeiites and some boninites to form what will become forearc crust. Magmatic products of a mature subduction zone manifest combination of a continuous flux of hydrous basalt from the mantle wedge, crustal magmatic process of fractionation and anatexis, and loss of dense pyroxene-rich cumulates from the base of the crust back to the mantle. The result of these processes is to produce crust that becomes increasingly felsic as it ages and slowly thickens. Mantle peridotites reflect these subduction-related asymmetries in melting and evolution: ultra-depleted harzburgites that are strongly serpentinized beneath the forearc, pyroxene-rich ultramafic rocks beneath the magmatic front, abyssal peridotite-like lherzolites and moderately depleted harzburgites beneath the back-arc basin. IOASs cannot be understood without understanding the remarkably different processes and magma production rates that accompany their early development. The characteristic dimensions and asymmetries of IOAS systems should be at least partly preserved in orogenic belts and discernible to careful observers.

This paper benefited from thoughtful reviews by M. Santosh and T. Kusky. Thanks go to E. Kohut for help with Fo–An relationships, and to A. Calvert for Figure 14. My research into the nature of intra-oceanic arc systems has been supported by the US National Science Foundation, most recently by OCE0405651. My studies of IOASs has benefited from many interactions with many colleagues in many ways over more than three decades. This is UTD Geosciences Department Contribution 1195.

References

Allan, J. F., Batiza, R. & Lonsdale, P. F. 1987. Petrology and chemistry of lavas from seamounts flanking the East Pacific Rise Axis, 21° N: implications concerning the mantle source composition for both Seamount and Adjacent EPR lavas. *In*: Keating, B., Fryer, P. F. & Batiza, R. (eds) *Seamounts, Islands, and Atolls*. American Geophysical Union, Geophysical Monograph, **43**, 255–282.

Arai, S. & Ishimaru, S. 2008. Insights into petrologic characteristics of the lithosphere of mantle wedge beneath arcs through peridotite xenoliths. A review. *Journal of Petrology*, **49**, 665–695.

Arculus, R. J. 2003. Use and abuse of the terms calcalkaline and calcalkalic. *Journal of Petrology*, **44**, 929–935.

Armstrong, R. L. 1991. The persistent myth of crustal growth. *Australian Journal of Earth Sciences*, **38**, 613–630.

Baker, E. T., Massoth, G. J., Nakamura, K. I., Embley, R. W., de Ronde, C. E. J. & Arculus, R. J.

2005. Hydrothermal activity on near-arc sections of back-arc ridges: results from the Mariana Trough and Lau Basin. *Geochemistry, Geophysics, Geosystems*, **6**, doi:10.1029/2005GC000948.

BAKER, E. T., EMBLEY, R. W. *ET AL.* 2008. Hydrothermal activity and volcano distribution along the Mariana arc. *Journal of Geophysical Research, Solid Earth*, **113**, doi:10.1029/2007JB005423.

BASALTIC VOLCANISM STUDY PROJECT (BVSP) 1981. Ocean-floor basaltic volcanism. *In*: BVSP (eds) *Basaltic Volcanism on the Terrestrial Planets*. Pergamon, Oxford, 132–160.

BEHN, M. D. & KELEMEN, P. B. 2006. Stability of arc lower crust: insights from the Talkeetna arc section, south central Alaska, and the seismic structure of modern arcs. *Journal of Geophysical Research, Solid Earth*, **111**, doi:10.1029/2006JB004327.

BLOOMER, S. H. & HAWKINS, J. W. 1983. Gabbroic and ultramafic rocks from the Mariana Trench: an island arc ophiolite. *In*: HAYES, D. E. (ed.) *The Tectonic and Geologic Evolution of Southeast Asian Seas and Islands: Part 2*. American Geophysical Union, Geophysical Monograph, **27**, 294–317.

BONATTI, E. & MICHAEL, P. J. 1989. Mantle peridotites from continental rifts to ocean basins to subduction zones. *Earth and Planetary Science Letters*, **91**, 297–311.

BROPHY, J. G. 2008. A study of Rare Earth Element (REE) – SiO_2 variations in felsic liquids generated by basalt fractionation and amphibolite melting: a potential test for discriminating between the two different processes. *Contributions to Mineralogy and Petrology*, **156**, 337–357.

CAGNIONCLE, A. M., PARMENTIER, W. M. & ELKINS-TANTON, L. T. 2007. Effect of solid flow above a subducting slab on water distribution and melting at convergent plate boundaries, *Journal of Geophysical Research, Solid Earth*, **112**, doi:10.1029/2007/JB004934.

CALVERT, A. J., KLEMPERER, S. L., TAKAHASHI, N. & KERR, B. C. 2008. Three-dimensional crustal structure of the Mariana island arc from seismic tomography. *Journal of Geophysical Research, Solid Earth*, **113**, doi:10.1029/2007JB004939.

CARR, M. J., SAGINOR, I. *ET AL.* 2007. Element fluxes from the volcanic front of Nicaragua and Costa Rica. *Geochemistry, Geophysics, Geosystems*, **8**, Q06001, doi:10.1029/2006GC001396.

CHAPP, E., TAYLOR, B., OAKLEY, A. & MOORE, G. F. 2008. A seismic stratigraphic analysis of Mariana forearc basin evolution. *Geochemistry, Geophysics, Geosystems*, **9**, doi:10.1029/2008GC001998.

CHRISTIENSEN, N. J. & MOONEY, W. D. 1995. Seismic velocity structure and composition of the continental crust: a global view. *Journal of Geophysical Research, Solid Earth*, **100**, 9761–9788.

CLIFT, P. & VANNUCCHI, P. 2004. Controls on tectonic accretion versus erosion in subduction zones: implications for the origins and recycling of the continental crust. *Reviews of Geophysics*, **42**, doi:10.1029/2003RG000127.

CLIFT, P. D., DRAUT, A. E., KELEMEN, P. B., BLUSZTAJN, J. & GREENE, A. 2005. Stratigraphic and geochemical evolution of an oceanic arc upper crustal section: the Jurassic Talkeetna Volcanic Formation, south-central Alaska. *Geological Society of America Bulletin*, **117**, 902–925.

COATS, R. R. 1962. Magma type and crustal structure in the Aleutian Arc. *In*: MCDONALD, G. A. & KUNO, H. (eds) *Crust of the Pacific Basin*. American Geophysical Union, Geophysical Monograph, **6**, 92–109.

CONDER, J. A., WIENS, D. A. & MORRIS, J. 2002. On the decompression melting structure at volcanic arcs and back-arc spreading centers. *Geophysical Research Letters*, **29**, doi:10.1029/2002GL015390.

D'ARS, J. B., JAUPART, C. & SPARKS, R. S. J. 1995. Distribution of volcanoes in active margins. *Journal of Geophysical Research, Solid Earth*, **100**, 20 421–20 432.

DAVIDSON, J. P. & ARCULUS, R. J. 2005. The significance of Phanerozoic arc magmatism in generating continental crust. *In*: BROWN, M. & RUSHMER, T. (eds) *Evolution and Differentiation of the Continental Crust*. Cambridge University Press, Cambridge, 135–172.

DAVIS, A. S. & CLAGUE, D. A. 1987. Geochemistry, mineralogy, and petrogenesis of basalt from the Gorda Ridge. *Journal of Geophysical Research, Solid Earth*, **92**, 10 476–10 483.

DEBARI, S. M., TAYLOR, B., SPENCER, K. & FUJIOKA, K. 1999. A trapped Philippine Sea plate origin for MORB from the inner slope of the Izu–Bonin trench. *Earth and Planetary Science Letters*, **174**, 183–197.

DEFANT, M. J. & DRUMMOND, M. S. 1990. Derivation of some modern arc magmas by melting of young subducted lithosphere. *Nature*, **347**, 662–665.

DE RONDE, C. E. J., MASSOTH, G. J., BAKER, E. T. & LUPTON, J. E. 2003. Submarine hydrothermal venting related to volcanic arcs. *In*: SIMMONS, S. F. & GRAHAM, I. (eds) *Volcanic, Geothermal, and Ore-forming Fluids: Rulers and Witnesses of Processes within the Earth*. Society of Economic Geologists Special Publication, **10**, 91–110.

DEWEY, J. F. & WINDLEY, B. F. 1981. Growth and differentiation of the continental crust. *Philosophical Transactions of the Royal Society of London, Series A*, **301**, 189–206.

DHUIME, B., BOSCH, D., BODINIER, J.-L., GARRIDO, C. J., BRUGUIER, O., HUSSAIN, S. S. & DAWOOD, H. 2007. Multistage evolution of the Jijal ultramafic–mafic complex (Kohistan, N Pakistan): implications for building the roots of island arcs. *Earth and Planetary Science Letters*, **261**, 179–200.

DICK, H. J. B. & BULLEN, T. 1984. Chromian spinels as a petrogenetic indicator in abyssal and alpine-type peridotites and spatially associated lavas. *Contributions to Mineralogy and Petrology*, **86**, 54–76.

DICKINSON, W. R. 1975. Potash–depth (K–*h*) relations in continental margins and intra-oceanic magmatic arcs. *Geology*, **3**, 53–56.

DILEK, Y. 2003. Ophiolite concept and its evolution. *In*: DILEK, Y. & NEWCOMB, S. (eds) *Ophiolite Concept and the Evolution of Geological Thought*. Geological Society of America, Special Papers, **373**, 1–16.

DIMALANTA, C., TAIRA, A., YUMUL, G. P. JR, TOKUYAMA, H. & MOCHIZUKI, K. 2002. New rates of western Pacific island arc magmatism from seismic and gravity data. *Earth and Planetary Science Letters*, **202**, 105–115.

Embley, R. W., Chadwick, W. W., Stern, R. J., Merle, S. G., Bloomer, S. H., Nakamura, K. & Tamura, Y. 2006. A synthesis of multibeam bathymetry and backscatter, and sidescan sonar of the Mariana submarine magmatic arc (abstract). *EOS Transactions, American Geophysical Union*, **87**, V41B-1723.

England, P., Engdahl, R. & Thatcher, W. 2004. Systematic variation in the depths of slabs beneath arc volcanoes. *Geophysical Journal International*, **156**, 377–408.

Fisher, R. L. & Engel, C. G. 1969. Ultramafic and basaltic rocks dredged from the nearshore flank of the Tonga Trench. *Geological Society of America Bulletin*, **80**, 1136–1141.

Fiske, R. S., Naka, J., Iizasa, K., Yuasa, M. & Klaus, A. 2001. Submarine silicic caldera at the front of the Izu–Bonin Arc, Japan: voluminous seafloor eruptions of rhyolite pumice. *Geological Society of America Bulletin*, **113**, 813–824.

Fliedner, M. M. & Klemperer, S. L. 2000. The transition from oceanic arc to continental arc in the crustal structure of the Aleutian Arc. *Earth and Planetary Science Letters*, **179**, 567–579.

Garcia, M. O., Pietruska, A. J., Rhodes, J. M. & Swanson, K. 2000. Magmatic processes during the prolonged Pu'u O'o eruption of Kilauea volcano, Hawaii. *Journal of Petrology*, **41**, 967–990.

Garfunkel, Z., Anderson, C. A. & Schubert, G. 1986. Mantle circulation and the lateral migration of subducted slabs. *Journal of Geophysical Research, Solid Earth*, **91**, 7205–7223.

Garrido, C. J., Bodinier, J.-L. *et al*. 2006. Petrogenesis of mafic garnet granulite in the lower crust of the Kohistan paleo-arc complex (northern Pakistan): implications for intra-crustal differentiation of island arcs and generation of continental crust. *Journal of Petrology*, **47**, 1873–1914.

Graham, I. J., Reyes, A. G., Wright, I. C., Peckett, K. M., Smith, I. E. M. & Arculus, R. J. 2008. Structure and petrology of newly discovered volcanic centers in the northern Kermadec–southern Tofua arc, South Pacific Ocean. *Journal of Geophysical Research, Solid Earth*, **113**, doi:10.1029/2007/JB005453.

Hacker, B. P., Peacock, S. M., Abers, G. A. & Holloway, S. D. 2003. Subduction factory 2. Are intermediate-depth earthquakes in subducting slabs linked to metamorphic dehydration reactions? *Journal of Geophysical Research, Solid Earth*, **108**, doi:10.1029/2001JB001129.

Hacker, B. R., Mehl, L., Kelemen, P. B., Rioux, M., Behn, M. D. & Luffi, P. 2008. Reconstruction of the Talkeetna intraoceanic arc of Alaska through thermobarometry. *Journal of Geophysical Research, Solid Earth*, **113**, doi:10.1029/2007JB005208.

Hamilton, W. 2007. Driving mechanism and 3-D circulation of plate tectonics. *In*: Sears, J. W., Harms, T. A. & Evenchick, C. A. (eds) *Whence the Mountains? Inquiries into the Evolution of Orogenic Systems: A Volume in Honor of Raymond A. Price*. Geological Society of America, Special Papers, **433**, 1–25.

Hamilton, W. B. 1988. Plate tectonics and island arcs. *Geological Society of America Bulletin*, **100**, 1503–1527.

Hawkesworth, C. J. & Kemp, A. I. S. 2006. Evolution of the continental crust. *Nature*, **443**, 811–817.

Hawkins, J. W., Bloomer, S. H., Evans, C. A. & Melchior, J. T. 1984. Evolution of intra-oceanic arc–trench systems. *Tectonophysics*, **102**, 175–205.

Herzburg, C. 2004. Geodynamic information in peridotite petrology. *Journal of Petrology*, **45**, 2507–2530.

Hofmann, A. W. 1988. Chemical differentiation of the Earth: the relationship between mantle, continental crust, and oceanic crust. *Earth and Planetary Science Letters*, **90**, 297–314.

Holbrook, W. S., Lizarralde, D., McGeary, S., Bangs, N. & Deibold, J. 1999. Structure and composition of the Aleutian island arc and implications for continental crustal growth. *Geology*, **27**, 31–34.

Jicha, B. R., Scholl, D. W., Singer, B. S., Yogodzinski, G. M. & Kay, S. M. 2006. Revised age of Aleutian Island Arc formation implies high rate of magma production. *Geology*, **34**, 661–664.

Jolly, W. T., Lidiak, E. G., Dickin, A. P. & Wu, T.-W. 2001. Secular geochemistry of central Puerto Rican island arc lavas: constraints on Mesozoic tectonism in the eastern Greater Antilles. *Journal of Petrology*, **42**, 2197–2214.

Jull, M. & Kelemen, P. B. 2001. On the conditions for lower crustal convective instability. *Journal of Geophysical Research, Solid Earth*, **106**, 6423–6446.

Kamimura, A., Kasahara, J., Shinohara, M., Hino, R., Shiobara, H., Fujie, G. & Kanazawa, T. 2002. Crustal structure study at the Izu–Bonin subduction zone around 31°N: implications of serpentinized materials along the subduction plate boundary. *Physics of the Earth and Planetary Interiors*, **132**, 105–129.

Karig, D. E. 1972. Remnant arcs. *Geological Society of America Bulletin*, **87**, 1057–1068.

Kelemen, P. B. 1995. Genesis of high Mg# andesites and the continental crust. *Contributions to Mineralogy and Petrology*, **120**, 1–19.

Kelemen, P. B., Hanghoj, K. & Greene, A. R. 2003. One view of the geochemistry of subduction-related magmatic arcs, with an emphasis on primitive andesite and lower crust. *In*: Rudnick, R. L. & Turekian, K. K. (eds) *Treatise of Geochemistry, 3*. Elsevier, Amsterdam, 593–659.

Kimura, J.-I. & Stern, R. J. 2008. Neogene volcanism of the Japan island arc: The K–*h* relationship revisited. *In*: Spencer, J. E. & Titley, S. R. (eds) *Circum-Pacific Tectonics, Geologic Evolution, and Ore Deposits*. Arizona Geological Society, Tucson, Digest, **22**, 187–202.

Kimura, J.-I. & Yoshida, T. 2006. Contributions of slab fluid, mantle wedge and crust to the origin of Quaternary lavas in the NE Japan Arc. *Journal of Petrology*, **47**, 2185–2232.

Kodaira, S., Sato, T., Takahashi, N., Ito, A., Tamura, Y., Tatsumi, Y. & Kaneda, Y. 2007. Seismological evidence for variable growth of crust along the Izu intra-oceanic arc. *Journal of Geophysical Research, Solid Earth*, **112**, doi:10.1029/2006JB004593.

Kusky, T. M., Glass, A. & Tucker, R. 2007. Structure, Cr-chemistry, and age of the Border Ranges ultramafic complex: a suprasubduction zone ophiolite. *In*: Ridgeway, K. D., Trop, J. M., Glen, J. M. G. & O'Neill, M. O. (eds) *Tectonic Growth of a Collisional Continental Margin: Crustal Evolution of Southern Alaska*. Geological Society of America, Special Papers, **431**, 207–225.

MARSAGLIA, K. 1995. Interarc and backarc basins. *In*: BUSBY, C. & INGERSOLL, R. V. (eds) *Tectonics of Sedimentary Basins*. Blackwell, Oxford, 299–329.

MARTINEZ, F. & TAYLOR, B. 2003. Controls on back-arc crustal accretion: insights from the Lau, Manus and Mariana basins. *In*: LARTER, R. D. & LEAT, P. T. (eds) *Intra-Oceanic Subduction Systems: Tectonic and Magmatic Processes*. Geological Society, London, Special Publications, **219**, 19–54.

MARTINEZ, F. & TAYLOR, B. 2006. Modes of crustal accretion in back arc basins: inferences from the Lau Basin. *In*: CHRISTIE, D. M., FISHER, C. R., LEE, S.-M. & GIVENS, S. (eds) *Back-Arc Spreading Systems: Geological, Biological, Chemical and Physical Interactions.* American Geophysical Union, Geophysical Monograph, **166**, 5–30.

NAKAJIMA, K. & ARIMA, M. 1998. Melting experiments on hydrous low-K tholeiite: implications for the genesis of tonalitic crust in the Izu–Bonin–Mariana arc. *Island Arc*, **7**, 359–373.

OAKLEY, A. J., TAYLOR, B., FRYER, P., MOORE, G. F., GOODLIFFE, A. M. & MORGAN, J. K. 2007. Emplacement, growth, and gravitational deformation of serpentinite seamounts on the Mariana forearc. *Geophysical Journal International*, **170**, 615–634.

OHARA, Y. 2006. Mantle process beneath Philippine Sea back-arc spreading ridges: a synthesis of peridotite petrology and tectonics. *Island Arc*, **15**, 119–129.

OHARA, Y., STERN, R. J., ISHII, T., YURIMOTO, H. & YAMAZAKI, T. 2002. Peridotites from the Mariana Trough backarc basin. *Contributions to Mineralogy and Petrology*, **143**, 1–18.

OKAMURA, H., ARAI, S. & KIM, Y. U. 2006. Petrology of forearc peridotite from the Hahajima Seamount, the Izu–Bonin arc, with special reference to the chemical characteristics of chromian spinel. *Mineralogical Magazine*, **70**, 15–26.

PARKINSON, I. J. & PEARCE, J. A. 1998. Peridotites from the Izu–Bonin–Mariana forearc (ODP Leg 125): evidence for mantle melting and melt-mantle interaction in a supra-subduction zone setting. *Journal of Petrology*, **39**, 1577–1618.

PEARCE, J. A. 2003. Subduction zone ophiolites: the search for modern analogues. *In*: DILEK, Y. & NEWCOMB, S. (eds) *Ophiolite Concept and the Evolution of Geological Thought*. Geological Society of America, Special Papers, **373**, 269–294.

PEARCE, J. A. & STERN, R. J. 2006. The origin of back-arc basin magmas: trace element and isotope perspectives. *In*: CHRISTIE, D. M., FISHER, C. R., LEE, S.-M. & GIVENS, S. (eds) *Back-Arc Spreading Systems: Geological, Biological, Chemical and Physical Interactions.* American Geophysical Union, Geophysical Monograph, **166**, 63–86.

PEARCE, J. A., BARKER, P. F., EDWARDS, S. J., PARKINSON, I. J. & LEAT, P. T. 2000. Geochemistry and tectonic significance of peridotites from the South Sandwich arc–basin system, South Atlantic. *Contributions to Mineralogy and Petrology*, **139**, 36–53.

PLANK, T. & LANGMUIR, C. H. 1988. An evaluation of the global variations in the major element chemistry of arc basalts. *Earth and Planetary Science Letters*, **90**, 349–370.

REAGAN, M. K., ISHIZUKA, O. *ET AL.* 2010. Fore-arc basalts and subduction initiation in the Izu–Bonin–Mariana system. *Geochemistry, Geophysics, Geosystems*, **11**, Q03X12, doi: 10.1029/2009GC002871.

RUDNICK, R. A. & GAO, S. 2003. Composition of the continental crust. *In*: RUDNICK, R. L. & TUREKIAN, K. K. (eds) *Treatise on Geochemistry, 3*. Elsevier, Amsterdam, 1–64.

SCHOLL, D. W. & VON HUENE, R. 2007. Crustal recycling at modern subduction zones applied to the past – issues of growth and preservation of continental basement, mantle geochemistry, and supercontinent reconstruction. *In*: HATCHER, R. D., CARLSON, M. P., MCBRIDE, J. H. & CATALAN, J. M. (eds) *The 4D Framework of Continental Crust*. Geological Society of America, Memoirs, **200**, 9–32.

SCHOLL, D. W. & VON HUENE, R. 2009. Implications of estimated magmatic additions and recycling losses at the subduction zones of accretionary (non-collisional) and collisional (suturing) orogens. *In*: CAWOOD, P. & KRÖNER, A. (eds) *Earth Accretionary Orogens in Space and Time*. Geological Society, London, Special Publications, **318**, 105–125.

SHAW, C. A., HEIZLER, M. T. & KARLSTROM, K. E. 2005. $^{40}Ar/^{39}Ar$ thermochronologic record of 1.45–1.35 Ga intracontinental tectonism in the southern Rocky Mountains: interplay of conductive and advective heating with intracontinental deformation. *In*: KARLSTROM, K. E. & KELLER, G. R. (eds) *The Rocky Mountain Region – An Evolving Lithosphere: Tectonics, Geochemistry, and Geophysics*. American Geophysical Union, Geophysical Monograph, **154**, 163–184.

SHILLINGTON, D. J., VAN AVENDONK, H. J. A., HOLBROOK, W. S., KELEMEN, P. B. & HORNBACH, M. J. 2004. Composition and structure of the central Aleutian island arc from arc-parallel wide-angle seismic data. *Geochemistry, Geophysics, Geosystems*, **5**, doi:10.1029/2004GC000715.

SHIPBOARD SCIENTIFIC PARTY 1982*a*. Site 455: east side of the Mariana Trough. *In*: HUSSONG, D. M., UYEDA, S. *ET AL.* (eds) *Initial Reports of the Deep Sea Drilling Project, Leg 60.* US Government Printing Office, Washington, DC, 203–213.

SHIPBOARD SCIENTIFIC PARTY 1982*b*. Site 458: Mariana fore-Arc. *In*: HUSSONG, D. M., UYEDA, S. *ET AL.* (eds) *Initial Reports of the Deep Sea Drilling Project, Leg 60.* US Government Printing Office, Washington, DC, 263–307.

STERN, R. J. 2002. Subduction zones. *Reviews of Geophysics*, **40**, doi:10.1029/2001RG000108.

STERN, R. J. 2004. Subduction initiation: spontaneous and induced. *Earth and Planetary Science Letters*, **226**, 275–292.

STERN, R. J. & BLOOMER, S. H. 1992. Subduction zone infancy: examples from the Eocene Izu–Bonin–Mariana and Jurassic California. *Geological Society of America Bulletin*, **104**, 1621–1636.

STERN, R. J. & SCHOLL, D. W. 2010. Yin and Yang of continental crust creation and destruction by plate tectonics. *International Geology Review*, **52**, 1–31.

STERN, R. J. & SMOOT, N. C. 1998. A bathymetric overview of the Mariana forearc. *Island Arc*, **7**, 525–540.

STERN, R. J., FOUCH, M. J. & KLEMPERER, S. 2003. An overview of the Izu–Bonin–Mariana subduction factory. *In*: EILER, J. (ed.) *Inside the Subduction*

Factory. American Geophysical Union, Geophysical Monograph, **138**, 175–222.

STERN, R. J., KOHUT, E., BLOOMER, S. H., LEYBOURNE, M., FOUCH, M. & VERVOORT, J. 2006. Subduction factory processes beneath the Guguan Cross-chain, Mariana Arc: no role for sediments, are serpentinites important? *Contributions to Mineralogy and Petrology*, **151**, 202–221.

STRAUB, S. M. 2003. The evolution of the Izu–Bonin–Mariana volcanic arcs (NW Pacific) in terms of major element chemistry. *Geochemistry, Geophysics, Geosystems*, **4**, doi:10.1029/2002GC000357.

SUYEHIRO, K., TAKAHASHI, N. *ET AL.* 1996. Continental crust, crustal underplating, and low-Q upper mantle beneath an oceanic island arc. *Science*, **272**, 390–392.

SYRACUSE, E. M. & ABERS, G. A. 2006. Global compilation of variations in slab depth beneath arc volcanoes and implications. *Geochemistry, Geophysics, Geosystems*, **7**, doi:10.1029/2005GC001045.

TAKAHASHI, N., KODAIRA, S., KLEMPERER, S. L., TATSUMI, Y., KANEDA, Y. & SUYEHIRO, K. 2007. Crustal structure and evolution of the Mariana intra-oceanic island arc. *Geology*, **35**, 203–206.

TAKAHASHI, N., KODAIRA, S., TASUMI, Y., KANEDA, Y. & SUYEHIRO, K. 2008. Structure and growth of the Izu–Bonin–Mariana arc crust: 1. Seismic constraint on crust and mantle structure of the Mariana arc–back-arc system. *Journal of Geophysical Research, Solid Earth*, **113**, doi:10.1029/2007JB005120.

TATSUMI, Y. 2005. The subduction factory: how it operates in the evolving Earth. *GSA Today*, **15**, 4–10.

TATSUMI, Y., SHUKUNO, H., TANI, K., TAKAHASHI, N., KODAIRA, S. & KOGISO, T. 2008. Structure and growth of the Izu–Bonin–Mariana arc crust: 2. Role of crust–mantle transformation and the transparent Moho in arc crust evolution. *Journal of Geophysical Research, Solid Earth*, **113**, doi:10.1029/2007JB005121.

WINDLEY, B. F. 1993. Uniformitarianism today: plate tectonics is the key to the past. *Journal of the Geological Society, London*, **150**, 7–19.

ZHAO, D., HASEGAWA, A. & KANAMORI, H. 1994. Deep structure of Japan subduction zone as derived from local, regional, and teleseismic events. *Journal of Geophysical Research, Solid Earth*, **99**, 22 313–22 329.